7 Kim HK, Silver B, Li S, et al: Hodgkin's disease in elderly patients (> or = 60): Clinical outcome and treatment strategies. Int J Radiat Oncol Biol Phys 2003;56:556–560.
8 Begg CB, Carbone PP: Clinical trials and drug toxicity in the elderly. The experience of the Eastern Cooperative Oncology Group. Cancer 1983;52:1986–1992.
9 Arias F, Duenas M, Martinez E, et al: Radical chemoradiotherapy for elderly patients with bladder carcinoma invading muscle. Cancer 1997;80:115–120.
10 Popescu RA, Norman A, Ross PJ, et al: Adjuvant or palliative chemotherapy for colorectal cancer in patients 70 years or older. J Clin Oncol 1999;17:2412–2418.
11 Pignon T, Gregor A, Schaake Koning C, et al: Age has no impact on acute and late toxicity of curative thoracic radiotherapy. Radiother Oncol 1998;46:239–248.
12 Sengelov L, Klintorp S, Havsteen H, et al: Treatment outcome following radiotherapy in elderly patients with bladder cancer. Radiother Oncol 1997;44:53–58.
13 Huguenin PU, Glanzmann C, Hammer F, Lutolf UM: Endometrial carcinoma in patients aged 75 years or older: Outcome and complications after postoperative radiotherapy or radiotherapy alone. Strahlenther Onkol 1992; 168:567–572.
14 Zachariah B, Balducci L: Radiation therapy of the older patient. Hematol Oncol Clin North Am 2000;14:131–167.
15 Pignon T, Horiot JC, Van den Bogaert W, et al: No age limit for radical radiotherapy in head and neck tumours. Eur J Cancer 1996; 32A:2075–2081.
16 Pignon T, Horiot JC, Bolla M, et al: Age is not a limiting factor for radical radiotherapy in pelvic malignancies. Radiother Oncol 1997;42: 107–120.
17 DiCarlo V, Balzano G, Zerbi A, Villa E: Pancreatic cancer resection in elderly patients. Br J Surg 1998;85:607–610.
18 Fong Y, Blumgart LH, Fortner JG, Brennan MF: Pancreatic or liver resection for malignancy is safe and effective for the elderly. Ann Surg 1995;222:426–434.
19 Hannoun L, Christophe M, Ribeiro J, et al: A report of forty-four instances of pancreaticoduodenal resection in patients more than seventy years of age. Surg Gynecol Obstet 1993; 177:556–560.
20 Hodul P, Tansey J, Golts E, et al: Age is not a contraindication to pancreaticoduodenectomy. Am Surg 2001;67:270–275; discussion 275–276.
21 Kayahara M, Nagakawa T, Ueno K, et al: Pancreatic resection for periampullary carcinoma in the elderly. Surg Today 1994;24:229–233.
22 Richter A, Schwab M, Lorenz D, et al: Surgical therapy of pancreatic carcinoma in elderly patients over 70. Langenbecks Arch Chir Suppl Kongressbd 1996;113:492–494.
23 Magistrelli P, Masetti R, Coppola R, et al: Pancreatic resection for periampullary cancer in elderly patients. Hepatogastroenterology 1998; 45:242–247.
24 Spencer MP, Sarr MG, Nagorney DM: Radical pancreatectomy for pancreatic cancer in the elderly. Is it safe and justified? Ann Surg 1990; 212:140–143.
25 Bathe OF, Levi D, Caldera H, et al: Radical resection of periampullary tumors in the elderly: Evaluation of long-term results. World J Surg 2000;24:353–358.
26 Miller AB, Hoogstraten B, Staquet M, Winkler A: Reporting results of cancer treatment. Cancer 1981;47:207–214.
27 Ikeda M, Okada S, Tokuuye K, et al: Prognostic factors in patients with locally advanced pancreatic carcinoma receiving chemoradiotherapy. Cancer 2001;91:490–495.
28 Kelsen DP, Portenoy R, Thaler H, et al: Pain as a predictor of outcome in patients with operable pancreatic carcinoma. Surgery 1997;122: 53–59.
29 Leichman CG: Prolonged infusion of fluorinated pyrimidines in gastrointestinal malignancies: A review of recent clinical trials. Cancer Invest 1994;12:166–175.
30 Poen JC, Collins HL, Niederhuber JE, et al: Chemo-radiotherapy for localized pancreatic cancer: Increased dose intensity and reduced acute toxicity with concomitant radiotherapy and protracted venous infusion 5-fluorouracil. Int J Radiat Oncol Biol Phys 1998;40:93–99.
31 Krzyzanowska MK, Weeks JC, Earle CC: Treatment of locally advanced pancreatic cancer in the real world: Population-based practices and effectiveness. J Clin Oncol 2003;21: 3409–3414.

Severe Drug Toxicity Associated with a Single-Nucleotide Polymorphism of the *Cytidine Deaminase* Gene in a Japanese Cancer Patient Treated with Gemcitabine plus Cisplatin

Kan Yonemori,[1] Hideki Ueno,[1] Takuji Okusaka,[1] Noboru Yamamoto,[2] Masafumi Ikeda,[1] Nagahiro Saijo,[2] Teruhiko Yoshida,[3] Hiroshi Ishii,[4] Junji Furuse,[4] Emiko Sugiyama,[5] Su-Ryang Kim,[5] Ruri Kikura-Hanajiri,[5] Ryuichi Hasegawa,[5] Yoshiro Saito,[5] Shogo Ozawa,[5] Nahoko Kaniwa,[5] and Jun-ichi Sawada[5]

Abstract

Purpose: We investigated single-nucleotide polymorphisms of the cytidine deaminase gene (*CDA*), which encodes an enzyme that metabolizes gemcitabine, to clarify the relationship between the single-nucleotide polymorphism 208G>A and the pharmacokinetics and toxicity of gemcitabine in cancer patients treated with gemcitabine plus cisplatin.

Experimental Design: Six Japanese cancer patients treated with gemcitabine plus cisplatin were examined. Plasma gemcitabine and its metabolite 2′,2′-difluorodeoxyuridine were measured using an high-performance liquid chromatography method, and the *CDA* genotypes were determined with DNA sequencing.

Results: One patient, a 45-year-old man with pancreatic carcinoma, showed severe hematologic and nonhematologic toxicities during the first course of chemotherapy with gemcitabine and cisplatin. The area under the concentration-time curve value of gemcitabine in this patient (54.54 μg hour/mL) was five times higher than the average value for five other patients (10.88 μg hour/mL) treated with gemcitabine plus cisplatin. The area under the concentration-time curve of 2′,2′-difluorodeoxyuridine in this patient (41.58 μg hour/mL) was less than the half of the average value of the five patients (106.13 μg hour/mL). This patient was found to be homozygous for 208A (Thr^{70}) in the *CDA* gene, whereas the other patients were homozygous for 208G (Ala^{70}).

Conclusion: Homozygous 208G>A alteration in *CDA* might have caused the severe drug toxicity experienced by a Japanese cancer patient treated with gemcitabine plus cisplatin.

Gemcitabine (2′,2′-difluorodeoxycytidine) is a deoxycytidine analogue that is efficacious against non–small cell lung cancer and pancreatic carcinoma, as a single agent or in platinum combination therapy (1, 2). Its major adverse effects are hematologic toxicity, weakness, and emesis, and its dose-limiting toxicity is hematologic toxicity, including leukocytopenia, anemia, and thrombocytopenia (1). Single-agent and platinum combination gemcitabine therapy is relatively well tolerated, but hospitalization is occasionally required due to significant hematologic toxicity (1, 2), and it has been difficult to predict the toxicity.

Gemcitabine is activated by intracellular phosphorylation to gemcitabine monophosphate by deoxycytidine kinase, which is subsequently phosphorylated to the higher-order phosphates, gemcitabine diphosphate followed by gemcitabine triphosphate. Gemcitabine triphosphate can be incorporated into DNA followed by one more deoxynucleotide, after which DNA polymerization stops. This process is referred to as "masked chain termination" (3, 4).

Gemcitabine and gemcitabine monophosphate are deaminated to the inactive metabolite 2′,2′-difluorodeoxyuridine (dFdU) and 2′,2′-difluorodeoxyuridine monophosphate by cytidine deaminase (CDA) and dCMP deaminase, respectively. Multiple mechanisms potentiate the activity of gemcitabine both by increased formation of active gemcitabine diphosphate and gemcitabine triphosphate and decreased elimination of gemcitabine, as follows: (a) gemcitabine diphosphate, through its inhibition of ribonucleotide reductase, depletes the deoxyribonucleotide pool available for DNA synthesis and repair; (b) the decreased concentration of dCTP activates deoxycytidine kinase, which accelerates phosphorylation of gemcitabine;

Authors' Affiliations: [1]Division of Hepatobiliary and Pancreatic Oncology and [2]Department of Medical Oncology, National Cancer Center Hospital; [3]Genetic Division, Research Institute, National Cancer Center, Tsukiji, Chuo-ku, Tokyo, Japan; [4]Division of Hepatobiliary and Pancreatic Oncology, National Cancer Center East Hospital, Kashiwanoha, Kashiwa, Chiba, Japan, and [5]NIH Sciences, Kamiyoga, Setagaya-ku, Tokyo, Japan

Received 7/29/04; revised 12/9/04; accepted 1/10/05.

Grant support: Program for the Promotion of Fundamental Studies in Health Sciences (MPJ-1 and MPJ-6) of the Pharmaceuticals and Medical Devices Agency of Japan (grants for the Millennium Genome Project from the Ministry of Health, Labor, and Welfare of Japan).

The costs of publication of this article were defrayed in part by the payment of page charges. This article must therefore be hereby marked *advertisement* in accordance with 18 U.S.C. Section 1734 solely to indicate this fact.

Requests for reprints: Kan Yonemori, Division of Hepatobiliary and Pancreatic Oncology, National Cancer Center Hospital, 5-1-1 Tsukiji, Chuo-ku, Tokyo 104-0045, Japan. Phone: 81-3-3542-2511; Fax: 81-3-3542-3815; E-mail: kyonemor@ncc.go.jp.

and (c) an inactivating enzyme, dCMP deaminase, is inhibited by the decreased concentration of intracellular dCTP and increased concentration of gemcitabine triphosphate (5-7). Polymorphisms of the DNAs encoding the above enzymes may influence the pharmacokinetics and pharmacodynamics of gemcitabine.

To establish the medical guidelines for treatment based on individual genetic polymorphisms, we have launched multicenter, prospective, pharmacogenomic trials (as the Millenium Genome Project) of antineoplastic agents, such as gemcitabine, paclitaxel, irinotecan, and other commonly used drugs.

At the time point when 97 gemcitabine-treated patients had been recruited, we experienced extremely severe toxicities in one patient. Because this patient was coadministered cisplatin in addition to gemcitabine, we compared the clinical data, pharmacokinetics and *CDA* genotype between this patient and the other five control patients, who were also coadministered the two drugs.

Patients and Methods

Selection of patients and treatment schedule. Patients being treated with gemcitabine plus cisplatin were eligible for the trial if they met all of the following inclusion criteria: histologically or cytologically proven carcinoma, no prior treatment with gemcitabine, age above 20 years, Eastern Cooperative Oncology Group performance status between 0 and 2, absence of severe infectious or neurologic disease, and no evidence of heart or interstitial lung disease. Other requirements included adequate bone marrow function (WBC ≥3,000/μL, neutrophils ≥1,500/μL, and platelets ≥75,000/μL), hepatic function (serum total bilirubin ≤3 mg/d, aspartate aminotransferase and alanine aminotransferase less than five times the upper limit of normal), and renal function (serum creatinine within the upper limit of normal). The trial was approved by the Ethics Review Committees of the National Cancer Center Hospital and NIH Sciences, and oral and written informed consent was obtained from all patients before entering.

Gemcitabine was given to all patients at a dose of 1,000 mg/m^2 (30-minute infusion) on days 1, 8, and 15 and followed by 1 week of rest. If adequate bone marrow function (WBC ≥2,000/μL, neutrophils ≥1,000/μL, and platelets ≥70,000/μL) was confirmed, gemcitabine was given on days 8 and 15.

Cisplatin was given at a dose of 80 mg/m^2 (150-minute infusion) on day 1, immediately after gemcitabine. All patients received antiemetic prophylaxis with granisetron plus dexamethasone. Granulocyte-colony stimulating factor was not given routinely. The treatment schedule was repeated every 28 days until disease progression or unacceptable side effects occurred.

Toxicity was scored according to the National Cancer Institute Common Toxicity Criteria ver 2.0. A complete blood cell count and serum chemistry were repeated weekly. At the start of every new course, the dose was reevaluated according to toxicity. If the WBC count was <2,000/μL and the platelet count was <70,000/μL, then treatment was delayed until the recovery of bone marrow function. If grade 4 leukocytopenia, neutrocytopenia, or thrombocytopenia was observed in the previous course, the gemcitabine dose was reduced to 800 mg/m^2 in subsequent courses.

Blood sampling. Before the start of the treatment, a 5-mL heparinized blood sample was collected to measure CDA activity, and a 14-mL blood sample, to which EDTA was added, was collected to extract leukocyte DNA for genetic analysis. On day 1 of the first course, a 5-mL heparinized blood sample for gemcitabine and metabolite analysis in plasma was collected from the opposite arm before the infusion, at 3 minutes before the end of the infusion, and 15, 30, 60, 90, 120, and 240 minutes after the end of the infusion, and 50 μL of 10 mg/mL tetrahydrouridine (Wako Junyaku, Co., Ltd., Osaka, Japan) was immediately added to each of the samples. The samples were centrifuged at 3,000 × *g* for 5 minutes at 4°C, and the plasma was collected and stored at −70°C until analyzed.

Analysis of gemcitabine and its metabolite, 2′,2′-difluorodeoxyuridine. The concentrations of gemcitabine and dFdU in the plasma were determined by the method of Venook et al. with slight modifications (8). A 25 μL volume of 25 mg/mL 3′-deoxy-3′-fluoro-thymidine (Aldrich Chem. Co., St. Louis, MO) was added to an 0.25-mL aliquot of plasma sample containing 0.1 mg/mL tetrahydrouridine as an internal standard. After adding 1 mL of acetonitrile, the mixtures were centrifuged at 12,000 × *g* for 5 minutes, and the supernatant was evaporated to dryness under a nitrogen stream. The residue was dissolved in 0.25 mL of 15 mmol/L ammonium acetate buffer (pH 5.0), and the solution was filtered twice through Ultrafree-MC (0.45 μm; Millipore Corp., Billerica, MA) and Microcon YM-10 (10,000 MW; Amicon). Twenty microliters of sample were loaded into a high-performance liquid chromatography system (HP 1100 model) with diode array detection and electrospray-mass spectrometry detection. The chromatographic conditions were as follows: column, CAPCELL PACK C18 MG column (5 μm, 2.0 × 150 mm; Shiseido Co., Ltd., Tokyo, Japan) with a CAPCELL C18 MG S-5 guard cartridge (4.6 mm i.d. × 10 mm; Shiseido); column temperature, 40°C; mobile phase, 15 mmol/L ammonium acetate (pH 5.0)/methanol; running program of the mobile phase: 95:5 (0 minute), −75:25 (10-15 minutes), −60:40 (20-25 minutes), − 95:5 (30-40 minutes); flow rate: 0.3 mL/min; diode array detection: 268 nm for gemcitabine, 258 nm for dFdU, and 266 nm for 3′-deoxy-3′-fluoro-thymidine; electrospray-mass spectrometry: *m/z* 264 for gemcitabine, *m/z* 265 for dFdU, and *m/z* 245 for 3′-deoxy-3′-fluoro-thymidine. Detection and integration of chromatographic peaks were done by the HP Chemistation data analysis system (Hewlett-Packard, Les Ulis, France).

Pharmacokinetic analysis. Compartment model independent pharmacokinetic variables were calculated using WinNonlin software, ver. 4.1 (Pharsight Co., Mountain View, CA). The values are expressed as means ± SD, except for those of the patient with severe toxicity.

DNA sequencing. DNA used for sequencing was extracted from peripheral blood. All of the four exons of *CDA* were amplified from 100 ng of genomic DNA using multiplex primers listed in Table 1 (PCR). The PCR conditions have been described previously (9). After the second amplification for each exon, the PCR products were purified and directly sequenced on both strands with the sequencing primers listed in Table 1 (sequencing), as described previously (9). All variations were confirmed by repeating the sequence analysis from the first-round PCR with DNA. National Center for Biotechnology Information accession no. NT_004610.16 was used for the reference sequence.

Table 1. Primer sequences used for the analysis of the human *CDA* gene

Region	Forward primer (5′-3′)	Reverse primer (5′-3′)
PCR		
Exon 1	TCCACCCTCCAATTGAGATA	AGTCGGCAGGGTAGGAACATTC
Exon 2	TTGATGGGACACATTCAGACCA	CCGCTTTATGTTTCAATGCTGC
Exon 3	CTCTTTGACCTTTGTATTCCC	TTGACTCAGAAACGCCACTGTT
Exon 4	GCACTATGATCCAGGTACAA	TCAGCTCTCCACACCATAAGG
Sequencing		
Exon 1	TGAGACAGGGTCTGGCTCTCTGT	GTGCTTCACACTCTCCCTTA
	CAGTAGCGTGGCACCACCTTCT	CGCCTCTTCCTGTACATCTT
	ATGGCCCAGAAGCGTCCT	GGCCCCAGACACGATTGC
Exon 2	CCACCTTGTTTGGAGTAACC	CTGGCACATAGGAAGTCCAC
	TGGGATGAGTGCTGAGGATA	TGTGTAAGGAAGATGTTGGC
Exon 3	CTTCAGGACACAGTGGATCT	TTCCAGTGACTCATGCAAGC
Exon 4	ATGGTCATTCCCCTTTTACA	GTCCCTCCTAAGAGCTGCAA
		AGGCTGGAGTGTAATCTGGA

Results

We encountered a patient treated with gemcitabine and cisplatin who developed extremely severe toxicities (grade 4 neutropenia, thrombocytopenia, and stomatitis and grade 3 rash, fatigue, and febrile neutropenia). To clarify the cause of these life-threatening toxicities, we determined the plasma levels of gemcitabine and its metabolite, dFdU, and the genotypes of *CDA* encoding a major gemcitabine-metabolizing enzyme, cytidine deaminase, of this patient (patient 1) and the other five gemcitabine/cisplatin-administered patients (patients 2-6).

Pharmacokinetics. Plasma concentration-time profiles of gemcitabine and dFdU are shown in Figs. 1 and 2, and pharmacokinetic variables are summarized in Table 2. The maximum plasma gemcitabine concentration (C_{max}) and area under the concentration-time curve of patient 1 were about twice and five times higher, respectively, than the average values of patients 2 to 6. In patient 1, gemcitabine clearance was decreased to one fifth of the average value of the other five cases, and the terminal phase half-life ($T_{1/2}$) of gemcitabine was four times longer than the average value in patients 2 to 6. The C_{max} and area under the concentration-time curve of dFdU in patient 1 were one third and one half, respectively, of the average values of patients 2 to 6. The area under the concentration-time curve ratio (dFdU/gemcitabine) of patient 1 was about one tenth of the average value in patients 2 to 6.

Genotypes. The results of *CDA* genotyping analysis are shown in Table 3. We only found three known single nucleotide polymorphisms (SNP) in the coding regions in these patients. Patient 1 was homozygous for 208G>A ($Ala^{70}Thr$) in exon 2 (10), but had homozygous wild-type alleles for the other SNPs in exons 1 and 4. All of the other patients carried the homozygous wild-type alleles in exon 2. Thus, it was assumed that the increased plasma gemcitabine levels in patient 1 might have been caused by the $Ala^{70}Thr$ substitution in cytidine deaminase.

Discussion

There was no nephrotoxicity or neurotoxicity in patient 1, which is specifically associated with cisplatin (11). In addition,

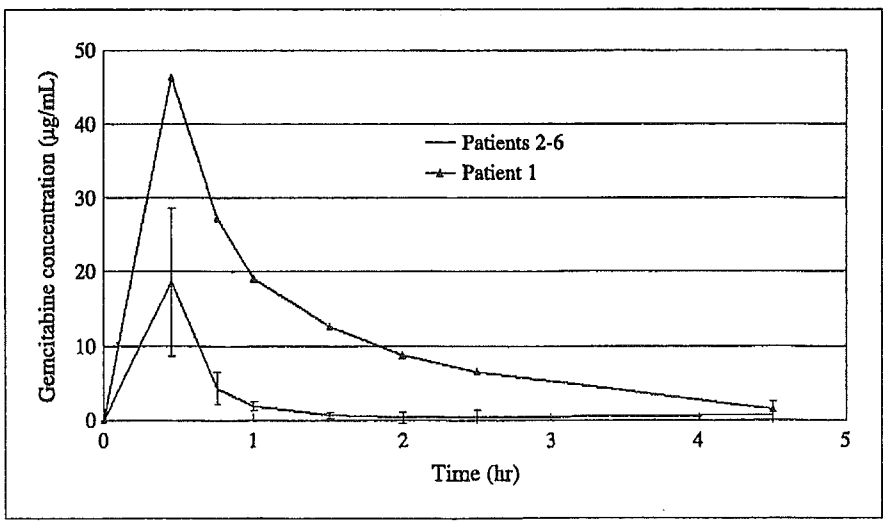

Fig. 1. Plasma disposition curve for gemcitabine in patient 1 (▲) and mean curve for patients 2 to 6 (*solid line*). Bars, SD.

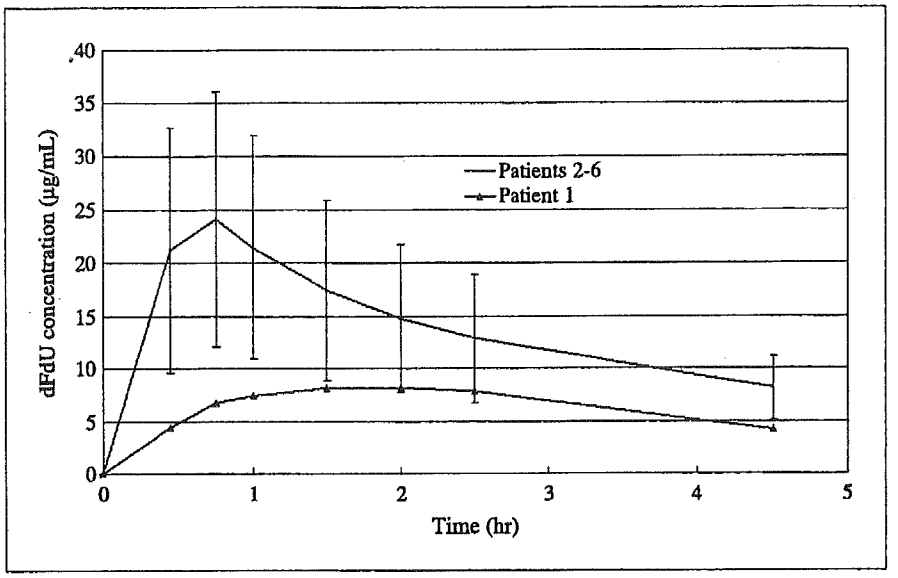

Fig. 2. Plasma disposition curve for dFdU in patient 1 (▲) and mean curve for patients 2 to 6 (*solid line*). Bars, SD.

the skin rash observed in patient 1 is common (with a reported 30.1% occurrence) in patients treated with gemcitabine in single-agent therapy (1). Therefore, we considered that the severe toxicity profile observed in patient 1 was mainly caused by the administration of gemcitabine.

Because the average pharmacokinetic profiles of gemcitabine and dFdU in patients 2 to 6 were almost the same as the population pharmacokinetic profiles in phase I and late phase II trials in Japan (12–14), the pharmacokinetic profiles of patients 2 to 6 can be regarded as standard for a Japanese population. Therefore, the plasma gemcitabine levels of patient 1 were remarkably high. Because the DLST of gemcitabine and cisplatin were negative in patient 1, the toxicities, especially a severe systemic rash including stomatitis and purpura, were unlikely to have been caused by drug allergies, such as Stevens-Johnson syndrome. Thus, the exposure to increased levels of gemcitabine is most likely responsible for the severe toxicities experienced in patient 1.

The patient backgrounds showed no major difference in age, body surface area, and performance status among patients with and without severe toxicities; age ranged from 45 to 69 years, the bovine serum albumin ranged from 1.42 to 1.78 m^2, and Eastern Cooperative Oncology Group performance status ranged from 0 to 1 (patient 1: 45 years, 1.78 m^2, performance status 0). None of the patients had received any prior chemotherapy or radiotherapy. It was unlikely that the patient backgrounds other than the *CDA* genotype caused the abnormal pharmacokinetics observed in patient 1.

Patient 1 was homozygous for the SNP 208G>A ($Ala^{70}Thr$), and all of the other patients carried the homozygous wild-type allele. Patient 1 carried no other known nonsynonymous and synonymous *CDA* polymorphisms (79A>C and 435C>T, respectively). The variant CDA enzyme with Thr^{70} was reported to show 40% and 32% of the activity of the wild-type for cytidine and 1-β-D-arabinofuranosylcytosine substrates in an *in vitro* experiment, respectively (10). Thus, the

Table 2. Compartment-independent pharmacokinetic variables of gemcitabine and its metabolite, dFdU

	Patient 1	Patients 2-6 (mean ± SD)
Gemcitabine		
C_{max} (μg/mL)	46.42	22.28 ± 5.08
AUC_{∞} (μg hour/mL)	54.54	10.88 ± 1.64
Cl (L per h per m^2)	18.34	93.17 ± 15.61
$T_{1/2}$ (h)	0.97	0.26 ± 0.03
V_z (L/m^2)	25.62	35.2 ± 7.47
dFdU		
C_{max} (μg/mL)	8.19	28.75 ± 4.09
AUC_{∞} (μg h/mL)	41.58	106.13 ± 31.44
Cl/F (L per h per m^2)	24.05	10.04 ± 2.98
$T_{1/2}$ (h)	2.17	2.46 ± 0.52
V_z (L/m^2)	75.4	34.29 ± 6.6
AUC ratio (dFdU/gemcitabine)	0.76	9.68 ± 2.05

Abbreviations: C_{max}, maximum plasma concentration; AUC_{∞}, area under the concentration-time curve; Cl, clearance; $T_{1/2}$, terminal-phase half-life; V_z = Dose / (λ_z × AUC); λ_z, elimination rate constant at terminal phase; *F*, metabolite fraction (*F* can be assumed to lie between 0.90 and 0.95).

Table 3. Genotypes of the three known polymorphic loci in exons of the *CDA* gene

Patient	Exon 1, 79A>C, K27Q	Exon 2, 208G>A, A70T	Exon 4, 435C>T, T145T (silent)
1	A/A	A/A	C/C
2	A/C	G/G	C/T
3	A/A	G/G	C/C
4	A/A	G/G	C/T
5	A/A	G/G	C/C
6	C/C	G/G	C/T

reduced activity of the variant enzyme with Thr^{70} might have resulted in the abnormal pharmacokinetics in patient 1.

The allelic frequency of the 208G>A polymorphism of the *CDA* gene in the Japanese population is 4.3% (10). Recently, genetic polymorphisms in the gemcitabine metabolic pathway, including *CDA* SNPs in Europeans and Africans, were reported by Fukunaga et al. (15). The SNP 208G>A was not detected in Europeans, whereas the allelic frequency of 208A was 0.125 in Africans (15). According to the two previous studies (10, 15), frequencies of homozygous 208G>A individuals in the Japanese and African populations were estimated to be about 0.18% and 1.56%, respectively. Therefore, severe toxicity caused by 208G>A could occur more frequently in Africans than in Japanese.

Based on the results of the analyses of the pharmacokinetic profiles and the 208G>A SNP, we can conclude that decreased CDA activity might have been responsible for the severe drug toxicity observed in this Japanese cancer patient.

Acknowledgments

We thank Emiko Jimbo and Miho Akimoto for assistance in sample collection and Atsuko Watanabe, Tomoko Chujo, Makiyo Iwamoto, and Mamiko Shimada for sample management.

References

1. Cortes-Funes H, Martin C, Abratt R, Lund B. Safty profile of gemcitabine, a novel anticancer agent, in non-small cell lung cancer. Anticancer Drugs 1997; 8:582–7.
2. Heinemann V, Wilke H, Mergenthaler HG, et al. Gemcitabine and cisplatin in the treatment of advanced or metastatic pancreatic cancer. Ann Oncol 2000;11: 1399–403.
3. Plunkett W, Huang P, Searcy CE, Gandhi V. Gemcitabine: preclinical pharmacology mechanisms of action. Semin Oncol 1996;23:3–15.
4. Heinemann V, Hertel LW, Grindey GB, Plunkett W. Comparison of the cellular pharmacokinetics and toxicity of 2′,2′-difluorodeoxycytidine and 1-β-D-arabinofuranosylcytosine. Cancer Res 1988;48:4024–31.
5. Huang P, Plunkett W. Induction of apotosis by gemcitabine. Semin Oncol 1995;22:19–25.
6. Heinemann V, Xu YZ, Chubb S, et al. Inhibition of ribonucleotide reduction in CCRF-CEM cells by 2′,2′-difluorodeoxycytidine. Mol Pharmacol 1990;38: 567–72.
7. Shewach DS, Reynolds KK, Hertel L. Nucleotide specificity of human deoxycytidine kinase. Mol Pharmacol 1992;42:518–24.
8. Venook AP, Egorin MJ, Rosner GL, et al. Phase I and pharmacokinetic trial of gemcitabine in patients with hepatic or renal dysfunction: Cancer and Leukemia Group B 9565. J Clin Oncol 2000;18:2780–7.
9. Nakamura T, Saito Y, Murayama N, et al. Apparent low frequency of sequence variability within the proximal promoter region of the cytochrome *P*450(CYP)3A5 gene in established cell lines from Japanese individuals. Biol Pharm Bull 2001;24:954–7.
10. Yue L, Saikawa Y, Ota K, et al. A functional single-nucleotide polymorphism in the human cytidine deaminase gene contributing to ara-C sensitivity. Pharmacogenetics 2003;13:29–38.
11. Johonson SW, Stevenson JP, O'Dwyer PJ. Pharmacology of cancer chemotherapy. In: De Vita VT, Hellman S, Rosenberg SA. Cancer principle and practice of oncology. 6th ed. Philadelphia: Lippincott William and Wilkins; 2001. p. 384–5.
12. Taguchi T, Furuse K, Fukuoka M, et al. LY188011 phase I study. Gan To Kagaku Ryoho 1996;23: 1011–8.
13. Fukuoka M, Negoro S, Kudo S, et al. Late phase II study of LY188011 in patient with non-small-cell lung cancer. GanTo Kagaku Ryoho 1996;23:1825–32.
14. Okada S, Ueno S, Okusaka T, Ikeda M, Furuse J, Maru Y. Phase I trial of gemcitabine in patients with advanced pancreatic cancer. Jpn J Clin Oncol 2001;31: 7–12.
15. Fukunaga AK, Marsh S, Murry DJ, Hurley TD, McLeod HL. Identification and analysis of single-nucleotide polymorphisms in the gemcitabine pharmacologic pathway. Pharmacogenomics J 2004;4: 307–14.

Possible Detection of Pancreatic Cancer by Plasma Protein Profiling

Kazufumi Honda,[1] Yasuharu Hayashida,[1,2] Tomoko Umaki,[1] Takuji Okusaka,[4] Tomoo Kosuge,[5] Satoru Kikuchi,[1,2] Mitsufumi Endo,[2] Akihiko Tsuchida,[2] Tatsuya Aoki,[2] Takao Itoi,[3] Fuminori Moriyasu,[3] Setsuo Hirohashi,[1] and Tesshi Yamada[1]

[1]Chemotherapy Division and Cancer Proteomics Project, National Cancer Center Research Institute; [2]Third Department of Surgery and [3]Fourth Department of Internal Medicine, Tokyo Medical University; and [4]Hepatobiliary and Pancreatic Oncology Division and [5]Hepatobiliary and Pancreatic Surgery Division, National Cancer Center Hospital, Tokyo, Japan

Abstract

The survival rate of pancreatic cancer patients is the lowest among those with common solid tumors, and early detection is one of the most feasible means of improving outcomes. We compared plasma proteomes between pancreatic cancer patients and sex- and age-matched healthy controls using surface-enhanced laser desorption/ionization coupled with hybrid quadrupole time-of-flight mass spectrometry. Proteomic spectra were generated from a total of 245 plasma samples obtained from two institutes. A discriminating proteomic pattern was extracted from a training cohort (71 pancreatic cancer patients and 71 healthy controls) using a support vector machine learning algorithm and was applied to two validation cohorts. We recognized a set of four mass peaks at 8,766, 17,272, 28,080, and 14,779 *m/z*, whose mean intensities differed significantly (Mann-Whitney *U* test, $P < 0.01$), as most accurately discriminating cancer patients from healthy controls in the training cohort [sensitivity of 97.2% (69 of 71), specificity of 94.4% (67 of 71), and area under the curve value of 0.978]. This set discriminated cancer patients in the first validation cohort with a sensitivity of 90.9% (30 of 33) and a specificity of 91.1% (41 of 45), and its discriminating capacity was further validated in an independent cohort at a second institution. When combined with CA19-9, 100% (29 of 29 patients) of pancreatic cancers, including early-stage (stages I and II) tumors, were detected. Although a multi-institutional large-scale study will be necessary to confirm clinical significance, the biomarker set identified in this study may be applicable to using plasma samples to diagnose pancreatic cancer. (Cancer Res 2005; 65(22): 10613-22)

Introduction

The 5-year survival rate of pancreatic cancer sufferers is the lowest among patients with common solid tumors. Pancreatic cancer is the fifth leading cause of cancer-related mortality in Japan and the fourth in the United States, with >19,000 estimated annual deaths in Japan and >28,000 in the United States (1–3). Pancreatic cancer is characterized by massive local invasion and early metastasis to the liver and regional lymph nodes. Because surgical resection is the only reliable curative treatment, early detection is essential to improve the outcomes of pancreatic cancer patients. However, the clinical symptoms of pancreatic cancer, except for obstructive jaundice, are often unremarkable until the advanced stages of the disease, and the anatomic location of the pancreas deep in the abdomen makes physical and ultrasonic detection of pancreatic cancer difficult. As a result, only 20% to 40% of pancreatic cancer patients undergo surgical resection (1, 4). Mass screening by computed tomography (CT), magnetic resonance imaging (MRI), or positron emission tomography (PET) may not be cost-effective because of the relatively low incidence of pancreatic cancer, and the long-term safety of these modalities has not been established (5). Thus, new diagnostic modalities allowing early detection of pancreatic cancer in a safe/noninvasive and cost-effective way are needed.

Recently, mass spectrometry (MS)–based proteomic approaches have gained considerable attention as effective modalities for identifying new biomarkers of various diseases because of their high sensitivity, but proteomic analysis of blood samples has been hampered by the marked dominance of a handful of particularly abundant proteins, including albumin, immunoglobulins, and transferrins (6). Surface-enhanced laser desorption/ionization (SELDI)-MS was developed to resolve these problems and is considered to be among the most useful tools available for the analysis of serum and plasma (7–9). Proteins are captured, concentrated, and purified on the small chemical surface of a SELDI chip, and the molecular weight (*m/z*) and relative intensity of each protein captured on the chip are measured with sensitive time-of-flight (TOF)-MS. As a result, a comprehensive proteomic profile can be created from as little as 20 μL serum/plasma samples. Combined with multivariate bioinformatical analysis, serum proteomics by SELDI-TOF-MS has been reported be successfully applied to the diagnosis of ovarian and prostate cancers (10–13).

The ProteinChip system is a sophisticated commercial platform designed for SELDI-TOF-MS. This system has been widely used because of its high-throughput automated measurements. However, relatively low resolution and poor mass accuracy have been recognized as drawbacks of the TOF-MS instrument of this system, and the reproducibility of SELDI-MS data has been controversial (14–16). Multivariate discrimination is dependent on stacks of small differences between cases and controls. Recently, Petricoin and Liotta reported the use of high-resolution performance hybrid quadrupole TOF-MS (QqTOF-MS) instruments to significantly improve the resolution and mass accuracy of SELDI-MS compared with results obtained with low-resolution instruments (17, 18).

Note: Supplementary data for this article are available at Cancer Research Online (http://cancerres.aacrjournals.org/).

Requests for reprints: Tesshi Yamada, Chemotherapy Division, National Cancer Center Research Institute, 5-1-1 Tsukiji Chuoh-ku, Tokyo 104-0045, Japan. Phone: 81-3-3547-5201, ext. 4270; Fax: 81-3-3547-6045; E-mail: tyamada@ncc.go.jp.

doi:10.1158/0008-5472.CAN-05-1851

Table 1. Clinicopathologic characteristics of the 220 cases seen at NCCH

	Training cohort			Validation cohort		
	Cancer (n = 71)	Healthy (n = 71)	P	Cancer (n = 33)	Healthy (n = 45)	P
Age (mean ± SD)	61.3 ± 9.06	62.1 ± 10.0	0.6*	62.0 ± 9.06	63.2 ± 11.7	0.6*
Gender						
Male	37	33	0.5†	18	24	0.92†
Female	34	38		15	21	
Tumor location						
Head	34			17		
Body or tail	37			10		
Unknown	0			6		
Clinical stage						
I	1			1		
II	6			4		
III	10			1		
IV	54			27		

*Student's t test.
†Fisher exact probability test.

Koopmann et al. (19) identified a set of biomarkers for pancreatic adenocarcinoma using the ProteinChip system. They increased the number of detectable peaks using stepwise anion-exchange chromatography, but only two of the six fractions were used for subsequent analyses. The two protein peaks that most effectively discriminated between pancreatic cancer patients and healthy controls reportedly achieved a sensitivity of 78% and a specificity of 97%, but this sensitivity was below the level necessary for clinical application. More importantly, diagnostic performance was not validated in an independent cohort. We reviewed and refined various aspects of SELDI-MS. In this study, we first compared the results obtained using low-resolution TOF-MS and high-resolution QqTOF-MS instruments and confirmed the high reproducibility of data obtained using the latter. Computerized machine learning may identify even a perfect multivariate classifier within a closed sample set in a nonbiological/mathematical way (16). Erroneous identification by machine learning must be eliminated by validation experiments using an independent sample set. Herein, we report the identification and validation of a set of biomarkers that can detect pancreatic cancer with high accuracy.

Materials and Methods

Patients and plasma samples. Plasma samples (n = 245) were obtained from two institutes, the National Cancer Center Hospital (NCCH; Tokyo, Japan) between August 2002 and October 2003 and the Tokyo Medical University Hospital (TMUH; Tokyo, Japan) between February 2004 and February 2005. The 220 NCCH cases included untreated pancreatic ductal adenocarcinoma patients (n = 104) and healthy controls (n = 116), whereas the 25 TMUH cases included untreated pancreatic ductal adenocarcinoma patients (n = 9), individuals with pancreatic tumors and/or cysts (n = 6), chronic pancreatitis patients (n = 5), and healthy controls (n = 5). The pancreatic tumor and/or cyst category included two pathologically unproven mucinous cystic tumors, two pathologically unproven serous

Table 2. Comparison of low-resolution and high-resolution instruments

	High-resolution QqTOF-MS		Low-resolution TOF-MS			
	Unfractionated		Unfractionated		Fractionated	
	No. unique peaks*	Correlation coefficient (r), mean ± SD	No. unique peaks*	Correlation coefficient (r), mean ± SD	No. unique peaks*	Correlation coefficient (r), mean ± SD
H50	263	0.96 ± 0.03	64	0.96 ± 0.04	214	0.76 ± 0.35
CM10 pH 4	124	0.99 ± 0.01	53	0.90 ± 0.11	219	0.73 ± 0.33
CM10 pH 7	73	0.98 ± 0.01	48	0.89 ± 0.09	168	0.61 ± 0.46
IMAC-Cu^{2-}	177	0.95 ± 0.04	61	0.87 ± 0.13	271	0.70 ± 0.44
Total	637		226		872	

*Number of unique peaks detectable in plasma samples from 24 pancreatic cancer patients and 24 healthy controls.

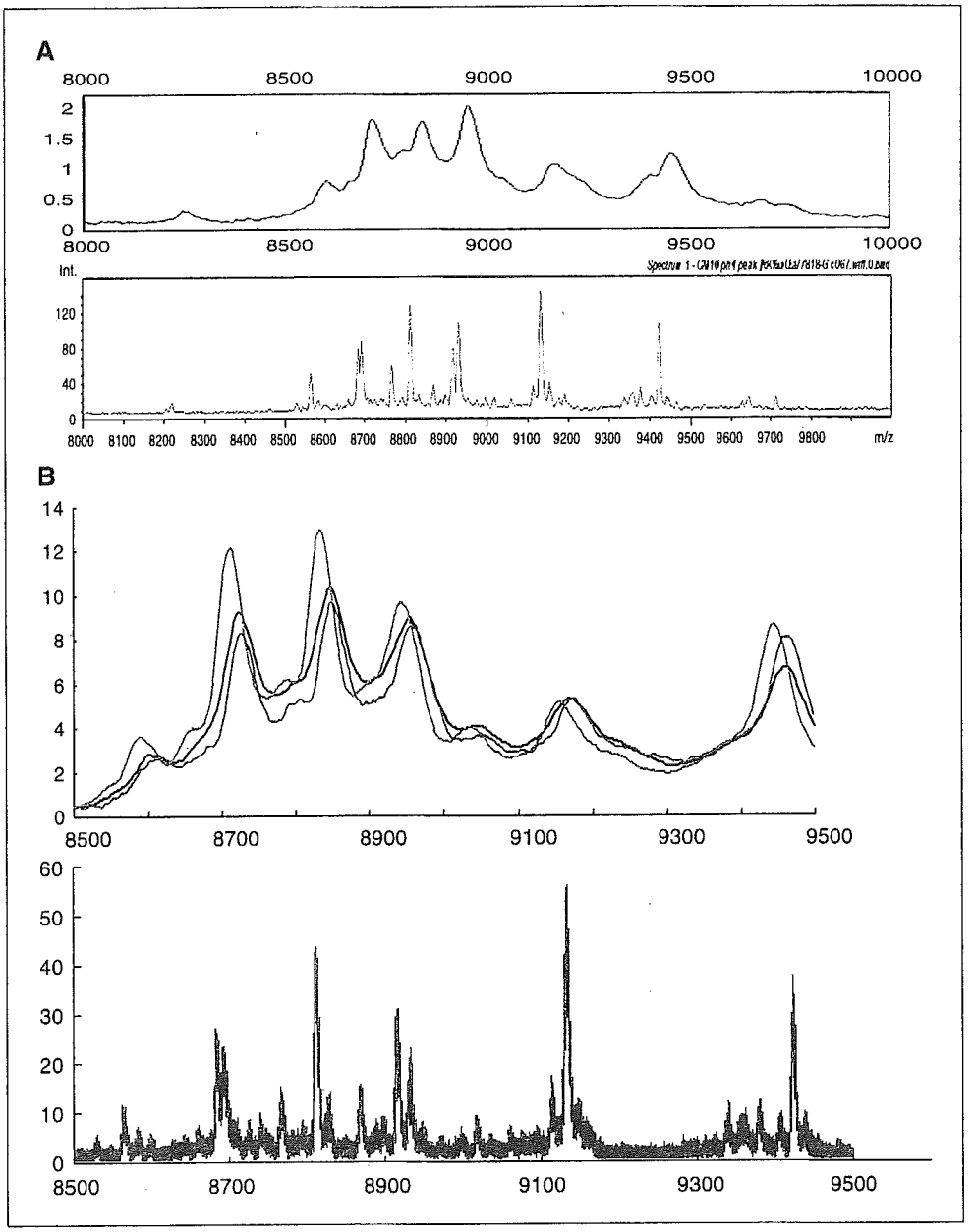

Figure 1. Comparison of low-resolution and high-resolution instruments. *A*, representative spectra of an unfractionated plasma sample in the range of 8,000 to 10,000 *m/z* obtained using a low-resolution TOF instrument (*top*) and a high-resolution QqTOF instrument (*bottom*). *B*, spectra of an unfractionated plasma sample in the range of 8,500 to 9,500 *m/z* obtained thrice every other day using a low-resolution TOF instrument (*top*) and a high-resolution QqTOF instrument (*bottom*). The spectra (*green*, *blue*, and *red lines*) were superimposed to allow visualization of the day-to-day variations. Note that only the *green line* is visible in the *bottom* because of the high reproducibility of results obtained with the QqTOF instrument.

papillary tumors, and two clinically diagnosed nonmalignant mass lesions in the pancreas. These cases are currently being followed, and a final diagnosis has not been obtained to date. The patients in the chronic pancreatitis category had no detectable mass lesions in the pancreas. Written informed consent was obtained from all of the subjects. Blood samples were collected in EDTA glass tubes. The supernatant was separated by centrifugation and cryopreserved at −80°C until analysis. All samples were processed in the same manner. The study was reviewed and approved by the ethics committees of the National Cancer Center (Tokyo, Japan; authorization nos. 16-36 and 16-71) and Tokyo Medical University (Tokyo, Japan; authorization no. 341).

The clinical characteristics of the patients are summarized in Table 1. Patients were classified as having clinical disease stage I, II, III, or IV according to the Fifth Edition of the General Rules for the Study of Pancreatic Cancer (Japanese Pancreas Society; ref. 20).

Surface-enhanced laser desorption/ionization. Ninety microliters of U9 buffer [9 mol/L urea, 2% 3-[(3-cholamidopropyl)dimethylammonio]-1-propanesulfonic acid, and 50 mmol/L Tris-HCl (pH 9)] were added to 10 μL of each plasma sample and vortexed for 20 minutes. Parts of the denatured plasma samples were fractionated using stepwise anion-exchange chromatography (pH 9 plus flow trough, pH 7, pH 5, pH 4, pH 3, and organic wash) with QHyper DF resin (Ciphergen Biosystems, Inc., Fremont, CA) using a Biomek 2000 Laboratory Automation Robot (Beckman Coulter, Fullerton, CA) according to a previously described method (12, 21).

Each sample was randomly assigned, with a 96-spot format, to 12 ProteinChip arrays (8 spots per array; Ciphergen) in duplicate using the Biomek 2000 Robot. Three types of ProteinChip arrays with different surface chemistries [i.e., immobilized metal affinity capture coupled with copper (IMAC-Cu^{2+}), weak hydrophobic (H50), or cationic (CM10) arrays] were used (21). The CM10 arrays were used under either low-stringent (pH 4) or high-stringent (pH 7) conditions as instructed by the supplier. The arrays were air-dried and applied to the matrix (50% sinapinic acid in 50% acetonitrile/0.1% trifluoroacetic acid).

Time-of-flight mass spectrometry. TOF-MS analysis was done using two types of mass spectrometers, a low-resolution TOF-MS (PBS IIc, Ciphergen) and a high-resolution QqTOF-MS [Q-star XL (Applied Biosystems, Framingham, CA) equipped with a PCI 1000 (Ciphergen)]. Peak detection for the low-resolution instrument was done using CiphergenExpress software

version 2.1 (Ciphergen). All of the spectra were compiled and normalized to the total ion currents, and the baselines were subtracted. Peaks between 3,000 and 30,000 *m/z* were autodetected using a signal-to-noise ratio of >3, and the peaks were clustered using second-pass peak selection with a signal-to-noise ratio of >2 and 0.3% mass windows. The permissible range of *m/z* drift between samples was set at 0.3% (21).

The high-resolution instrument was set to measure the range between 2,000 and 40,000 *m/z*. The laser intensity, laser frequency, and accumulation time were set to 60%, 25 Hz, and 90 seconds, respectively. The mass data obtained using the high-resolution instrument were converted to text files consisting of *m/z* and intensity after mass calibration by Analyst QS (Applied Biosystems) and were processed using newly developed in-house peak detection, normalization, and quantification software (22).

The peak data were visualized using Mass Navigator software (Mitsui Knowledge Industry, Tokyo, Japan). Mass accuracy was calibrated externally on the day of the measurements using an all-in-one-peptide molecular mass standard (Ciphergen).

Statistical analysis. Statistically significant differences were detected using the Fisher exact probability test, the Student's *t* test, and the Mann-Whitney *U* test. Receiver operator characteristics (ROC) curves were generated and the area under the curve (AUC) values were calculated using StatFlex software version 5.0 (Artech, Osaka, Japan; ref. 23).

We compiled the multivariate intensity data of the mass peaks into the distance from a support vector machine (SVM) hyperplane using the following formula (details in Supplementary Data; ref. 24):

$$dis(x_i) = \sum_{j=1}^{N} \lambda_j y_j \{k(x_j, x_i) + \alpha\}$$

where y_i is label (1 or -1), $k(x_j,x_i)$ is Gaussian kernel function, and λ_i is a value that maximizes [1] target function under [2] constrained conditions, where $L = \sum_{i=1}^{N} \lambda_i - \frac{1}{2} \sum_{i=1}^{N} \sum_{j=1}^{N} \lambda_i \lambda_j y_i y_j K(x_i, x_j)$ is the [1] target function, $0 \le \lambda_i \le C \sum_{i=1}^{N} \lambda_i y_i = 0$ are the [2] constrained conditions, and α and C are constants 0.25 and 10, respectively.

Immunoradiometric assay of CA19-9. Plasma (100 μL) was analyzed using a commercially available immunoradiometric assay kit (Fujirebio Diag-nostic, Inc., Malvern, PA) according to the manufacturer's recommendations.

Results

Comparison between low-resolution and high-resolution instruments. The reproducibility of data obtained using the low-resolution TOF-MS instrument of the ProteinChip system has been a concern. We compared the number of detectable peaks and the reproducibility of data obtained using low-resolution TOF-MS and high-resolution QqTOF-MS instruments. From unfractionated plasma samples (24 pancreatic cancer patients and 24 healthy controls), a total of 226 unique peaks were detected using the low-resolution instrument and 637 unique peaks were detected using the high-resolution instrument (Table 2). This difference seems to be attributable to the mass resolutions of the instruments (Fig. 1*A*). In addition, we noticed significant mass drifts (<0.3%) in the data obtained with the low-resolution instrument (Fig. 1*B*). In contrast, the mass deviation was <0.05% for the high-resolution instrument (Fig. 1*B*). As a result, the correlation coefficients for three independent measurements of a pooled plasma sample done every other day with the high-resolution instrument reached 0.97 to 0.99 (data not shown).

Chromatographic fractionation reduced the reproducibility of measurements. Fractionation via stepwise anion-exchange chromatography has been widely done to increase the number of detectable peaks obtained with low-resolution instruments. Actually, the total number of detectable peaks increased from 226 to 872 with fractionation of the same plasma samples (Table 2). However, the fractionation procedure seemed to compromise the reproducibility of the measurements. Forty-eight plasma samples (24 pancreatic cancer patients and 24 healthy controls) were analyzed in duplicate, and the mean correlation coefficient of all the peaks calculated between the duplicates was 0.87 to 0.96 for the unfractionated samples and 0.61 to 0.76 for the fractionated samples (Table 2). Fig. 2*A* (unfractionated) and Fig. 2*B* (fractionated) show the results of duplicate assays of a representative plasma sample.

Based on these quality-control experiments, we decided to measure unfractionated plasma samples using the high-resolution QqTOF-MS instrument. More than 90% of the duplicate

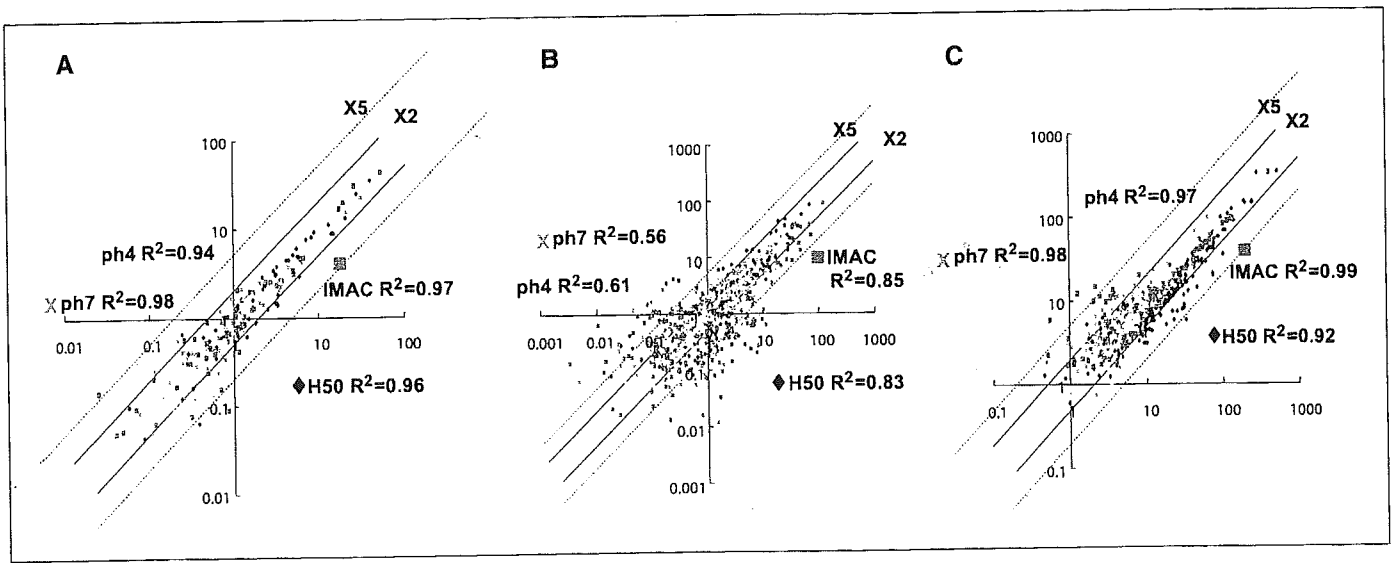

Figure 2. Reproducibility of data from the low-resolution and high-resolution instruments. Two-dimensional plot analyses of the mass intensities corresponding to the duplicated peaks that appeared in the H50 (*blue diamonds*), IMAC-Cu^{2+} (*red squares*), CM10 pH 4 (*yellow triangles*), and CM10 pH 7 (*light blue crosses*) arrays. Unfractionated (*A* and *C*) or fractionated (*B*) samples of the same plasma were measured using a low-resolution TOF instrument (*A* and *B*) and a high-resolution QqTOF instrument (*C*).

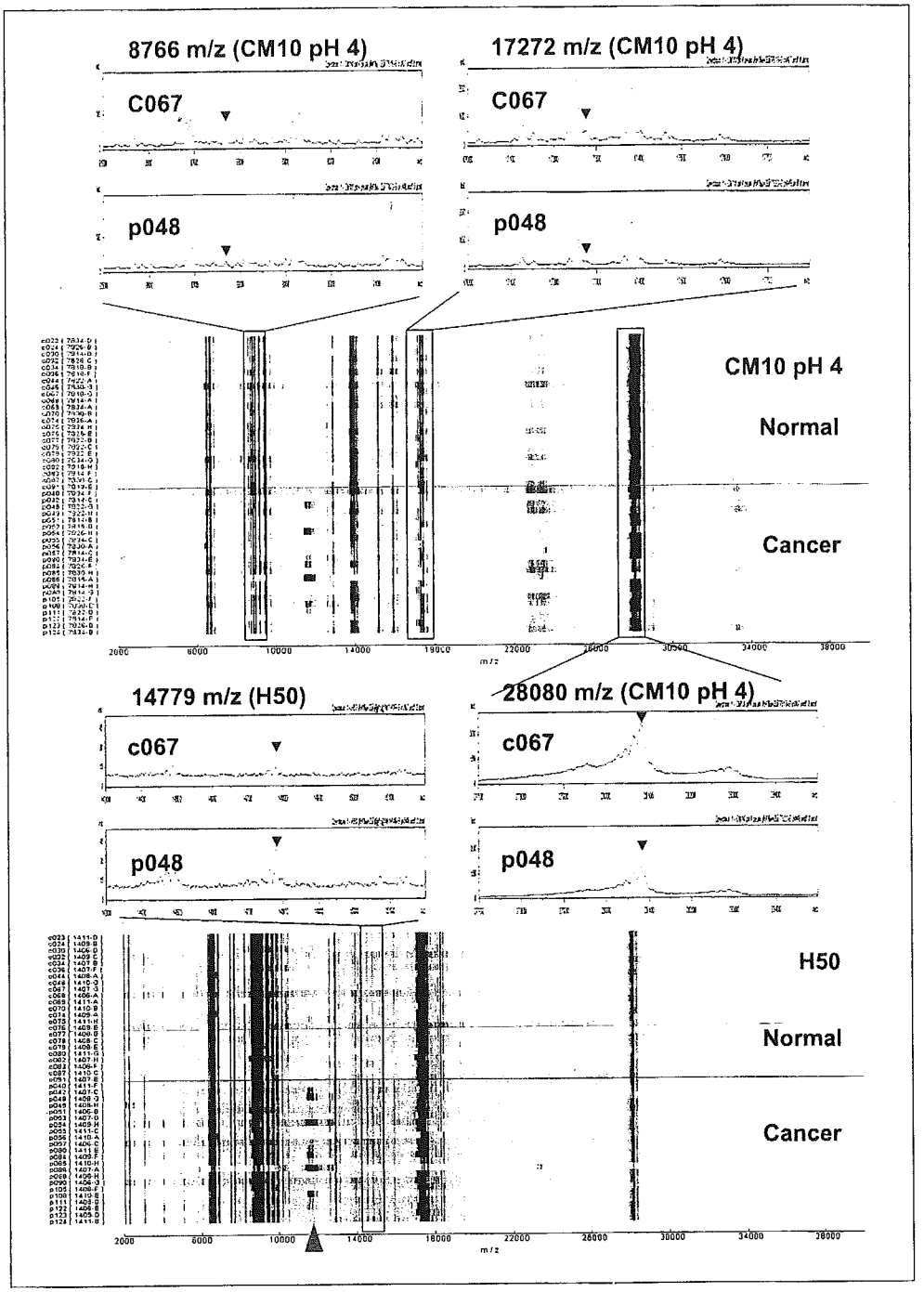

Figure 3. Representative mass spectra [a healthy control (*c067*) and a pancreatic cancer patient (*p048*)] and converted gel-like images [23 healthy controls (*c023-c091*) and 22 pancreatic cancer patients (*p040-p124*)] showing the peaks at 8,766, 17,272, 28,080 (CM10 pH 4), and 14,779 (H50) *m/z*. *Red arrowhead*, peak at 11,516 *m/z*, which was extracted using the Akaike information criterion (25).

protein peaks measured with the QqTOF-MS instrument were plotted within a 2-fold difference (Fig. 2*C*), and the mean correlation coefficient between duplicate assays was at least 0.95 (Table 2).

Identification of a candidate classifier in the training cohort by machine learning. From the total of 220 samples obtained at the NCCH, we selected 71 pancreatic cancer patients and 71 healthy controls with no statistically significant differences in age or sex distribution as a training cohort (Table 1). The remaining 78 cases served as a validation cohort. The clinicopathologic characteristics of these pancreatic cancer patients in the training and validation cohorts are summarized in Table 1.

The acquired MS peak information was stored in a large-capacity server computer, and the data set that most accurately discriminated pancreatic cancer patients from healthy controls was extracted using a rbf SVM learning algorithm (24). The set, or classifier, was composed of four protein peaks at 17,272 *m/z* (CM10 pH 4), 8,766 *m/z* (CM10 pH 4), 28,080 *m/z* (CM10 pH 4), and 14,779 *m/z* (H50). The selection of these four peaks was evaluated by leave-one-out (LOO) cross-validation. Representative spectra profiles and pseudo-gel images of the four peaks are shown in Fig. 3. Akaike information criterion procedure (25) selected another peak at 11,516 *m/z* (H50; indicated by a *red arrowhead* in Fig. 3). Although the 11,516 *m/z* peak was only

Table 3. Intensities of the 17,272, 8,766, 14,779, and 28,080 *m/z* peaks

Peaks (arrays)	Training cohort (n = 142)			Validation cohort (n = 78)		
	Cancer (n = 71)	Healthy (n = 71)	P*	Cancer (n = 33)	Healthy (n = 45)	P*
17,272 *m/z* (CM10 pH 4)	9.49 ± 2.88†	14.6 ± 2.29†	0.0000	9.74 ± 4.22†	14.5 ± 2.29†	0.0000
8,766 *m/z* (CM10 pH 4)	7.65 ± 3.53†	12.1 ± 5.55†	0.0000	7.04 ± 4.39†	13.4 ± 5.81†	0.0000
14,779 *m/z* (H50)	11.8 ± 4.43†	7.85 ± 3.68†	0.0000	10.4 ± 3.85†	6.46 ± 1.63†	0.00000
28,080 *m/z* (CM10 pH 4)	113 ± 36.7†	132 ± 33.5†	0.0022	92.4 ± 24.3†	110 ± 21.6†	0.0078

*Mann-Whitney *U* test.
†Mean ± SD intensities in arbitrary units.

detected in 1 of the 71 (1.4%) healthy controls, it was not included in the above discriminating data set generated by machine learning because of its low-positive rate in pancreatic cancer patients [19.7% (14 of 71)].

Statistical differences in all four peaks were recognized between the pancreatic cancer patients and the healthy controls (Mann-Whitney *U* test, $P < 0.0022$; Table 3). The ROC and AUC values of each peak and their combination in the 142 cases of the training cohort are shown in Fig. 4.

The intensity data of the four peaks obtained in each individual were compiled into a single value, the distance from a fixed SVM hyperplane, using the formula described in Materials and Methods and Supplementary Data. When the distance was positive, the individual was classified as having pancreatic cancer and vice versa. This classifier correctly diagnosed 97.2% (69 of 71) of the cancer patients and 94.4% (67 of 71) of the healthy controls in the training cohort (Fig. 5*A*).

Confirmation of the classifier in the first validation cohort. We next validated the discriminating performance of the classifier in a blinded manner using an independent cohort consisting of 78 individuals (NCCH) who had not been included in the training cohort (Table 1). Again, statistically significant differences in the mean intensities of every peak were observed between the 33 pancreatic cancer patients and the 45 healthy controls (Mann-Whitney *U* test, $P < 0.0078$; Table 3).

The SVM hyperplane determined in the training cohort was applied to the diagnosis of the 78 cases in the validation set. The same SVM hyperplane separated 90.9% (30 of 33) of the pancreatic cancer patients into the positive direction group and 91.1% (41 of 45) of the healthy controls into the negative direction group (Fig. 5*B*). The overall accuracy of the classification was 91.0% (71 of 78) in the validation cohort.

Combination of the surface-enhanced laser desorption/ionization classifier and CA19-9. Overall, the classifier was able to detect 95.2% (99 of 104) of the pancreatic cancer patients in the training and validation cohorts (Table 4). Although the number of cases was small, 83.3% (10 of 12) of stage I and II cases were detected (training and first validation cohorts). No statistically significant differences in detection rates were seen among cases with different tumor locations or different clinical stages (Table 4). To improve the detection rate, we measured plasma CA19-9 levels in all individuals whose residual samples were sufficient (29 pancreatic cancer patients and 39 healthy controls; Table 5). The sensitivity of CA19-9 (cutoff value of 37 units/mL) was 86.2% (25 of 29) and specificity was 94.9% (37 of 39). The SELDI classifier and the CA19-9 level were complementary. Combining CA19-9 and the SELDI classifier detected 100% (29 of 29) of cancer patients, but this combination yielded six false-positive cases [15.4% (6 of 39); Table 5].

Confirmation of the classifier in a second validation cohort obtained at a different institution. Finally, we did a second confirmatory experiment using samples collected prospectively at another institution. In total, 25 plasma samples from pancreatic cancer patients, individuals with other pancreatic diseases, and healthy volunteers were obtained from TMUH and analyzed in a blinded manner. Although the discovery of biomarkers useful for the differential diagnosis of pancreatic diseases was not the primary goal of this study, the classifier was able to discriminate pancreatic cancer patients and individuals with pancreatic tumors/cysts from healthy controls and pancreatitis patients (Table 4; Fig. 6). Four of the six patients with pathologically unproven pancreatic tumors/cysts were classified into the positive direction group. A close follow-up of these patients has been undertaken, because they may have premalignant or preclinical conditions. The SELDI classifier correctly identified 88.9% (8 of 9)

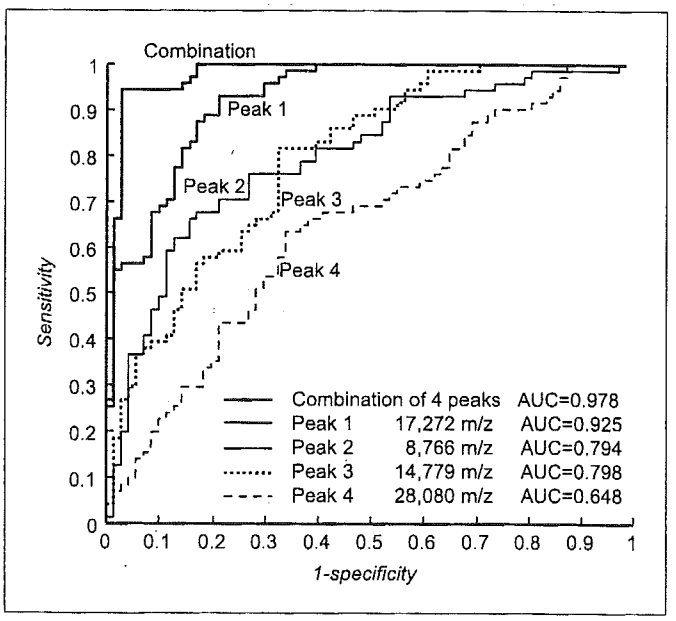

Figure 4. ROC curves and AUC values showing the discriminating capacities of the 17,272, 8,766, 28,080 (CM10 pH 4), and 14,779 (H50) *m/z* peaks individually and in combination.

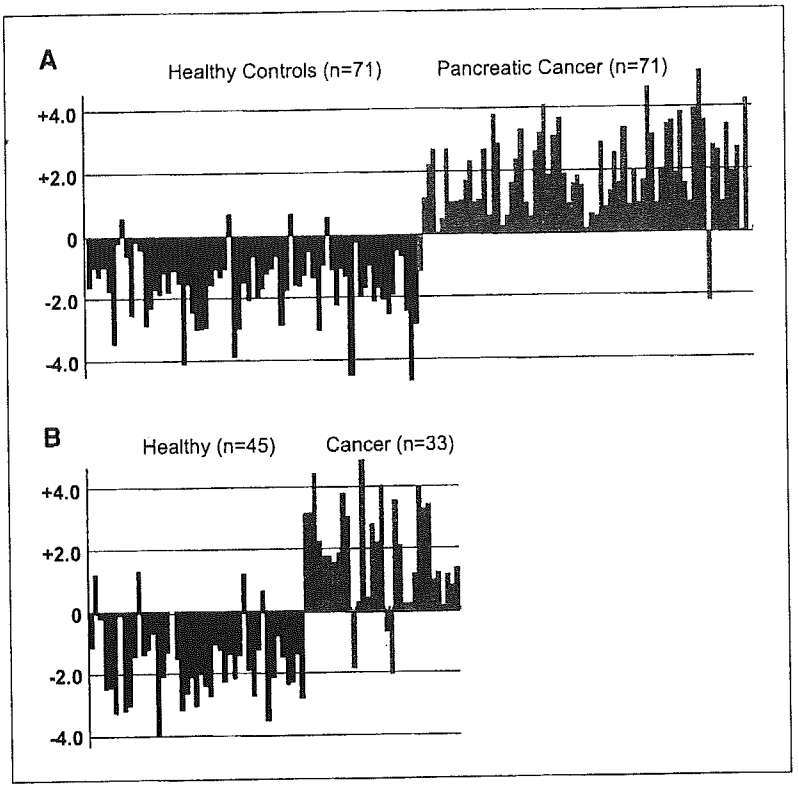

Figure 5. Calculated SVM distances of healthy controls (*black columns*) and pancreatic cancer patients (*gray columns*) in the training (*A*) and first validation (*B*) cohorts. Cases separated into the positive direction from the SVM hyperplane were classified as having "cancer" and those separated into the negative direction were classified as being "healthy."

of the pancreatic cancer patients and 80% (4 of 5) of the healthy controls, whereas the CA19-9 level correctly identified 66.7% (6 of 9) of the pancreatic cancer patients and 100% (5 of 5) of the healthy controls (Fig. 6). Again, in all the pancreatic cancer patients (9 of 9), the SELDI classifier and the CA19-9 level provided complementary results, even in this second validation cohort.

Discussion

Comparative proteomic profiling coupled with a computerized machine learning approach may revolutionize medical practice and cancer diagnosis. We compared the plasma protein profiles of a large number of pancreatic cancer patients and healthy controls with identical age and gender distributions (Table 1) to identify a biomarker for detecting pancreatic cancer patients in a large

Table 4. Diagnostic accuracy of the SELDI classifier

	Training cohort		Validation cohort (NCCH)		Validation cohort (TMUH)	
	No. cases	No. correctly classified samples* (%)	No. cases	No. correctly classified samples* (%)	No. cases	No. correctly classified samples* (%)
Healthy	71	67 (94.4)	45	41 (91.1)	5	4 (80)
Pancreatitis					5	4 (80)
Tumor/cyst†					6	4 (66.6)
Cancer	71	69 (97.2)	33	30 (90.9)	9	8 (88.9)
Cancer location						
Head	34	33 (97.1)	17	14 (82.4)	7	7 (100)
Body or tail	37	36 (97.3)	10	10 (100)	2	1 (50)
Unknown	0	0	6	10 (100)		
Clinical stage						
I	1	0 (0)	1	1 (100)	0	0
II	6	6 (100)	4	3 (75)	0	0
III	10	9 (90)	1	1 (100)	3	3 (100)
IV	54	54 (100)	27	25 (92.6)	6	5 (83.3)

*Number of healthy and chronic pancreatitis cases, considered to be "healthy," and number of pancreatic tumor/cyst and cancer cases given a diagnosis of "cancer."
†Pathologically unproven pancreatic tumor and/or cyst.

Table 5. Detection rates with CA19-9, the SELDI classifier, and their combination

	No. cases*	CA19-9, *n* (%)	SELDI, *n* (%)	Combination, *n* (%)
Healthy	39	3 (7.7)	4 (10.3)	6 (15.4)
Cancer	29	25 (86.2)	26 (89.7)	29 (100)
Clinical stage				
I	1	1 (100)	1 (100)	1 (100)
II	3	3 (100)	2 (66.6)	3 (100)
III	1	0 (0)	1 (100)	1 (100)
IV	24	21 (87.5)	22 (91.7)	24 (100)

*Cases whose plasma samples were available for CA19-9 measurement in the NCCH validation cohort.

population composed mainly of healthy individuals. The reproducibility of data obtained using the low-resolution instrument of the ProteinChip system has been a concern, but employing a high-resolution QqTOF instrument was found to significantly improve mass accuracy and minimize day-to-day variations (Fig. 1*B*). The high reproducibility of measurements was confirmed not by using a few high-intensity peaks selected intentionally but rather by using all the peaks detectable in the entire range (intensity and *m/z*) of mass spectra (Fig. 2). We also eliminated fractionation procedures, which increased the number of detectable peaks but significantly decreased reproducibility (Table 2; Fig. 2). A minimal set of four low-molecular weight proteins (Fig. 3) was found to be sufficient for discriminating pancreatic cancer patients with a sensitivity of 97.2% (69 of 71) and a specificity of 94.4% (67 of 71; Fig. 5*A*). This high discriminating capacity was confirmed by LOO cross-validation and ROC analysis (Fig. 4). We confirmed the discriminating capacity of our classifier in two independent validation cohorts (Figs. 5*B* and 6) to eliminate accidental identification of nonbiological/mathematical multivariate classifiers within a closed cohort by overfitting.

We noticed that a peak at 11,516 *m/z* (H50) was detected in 19.4% of the pancreatic cancer patients in the training cohort but in only 1.4% of the healthy controls (the peaks are indicated by a *red arrowhead* in Fig. 3). Tolson et al. (26) reported that an 11.5-kDa protein was detected in 32% of renal cell carcinoma patients but in none of the normal controls. Howard et al. (27) identified 11,682 *m/z* proteins in the sera of lung cancer patients as a diagnostic biomarker using matrix-assisted laser desorption/ionization (MALDI)-TOF-MS. Both groups identified the proteins as fragments of serum amyloid A. Serum amyloid A is an acute-phase reactant and a biomarker for inflammatory disease. The serum amyloid A level is elevated up to 1,000-fold during tissue damage and inflammation and is also increased in patients with various solid tumors and hematopoietic malignancies. However, serum amyloid A has not been recognized as a tumor marker because of its low positive rate (28, 29). Consistently, the 11,516 *m/z* peak was not incorporated into our classifier. The discovery of a single biomarker differing markedly between cancer patients and controls as well as having a high positive rate in cancer patients would be ideal but is perhaps not realistic. Since the discovery of CA19-9 in

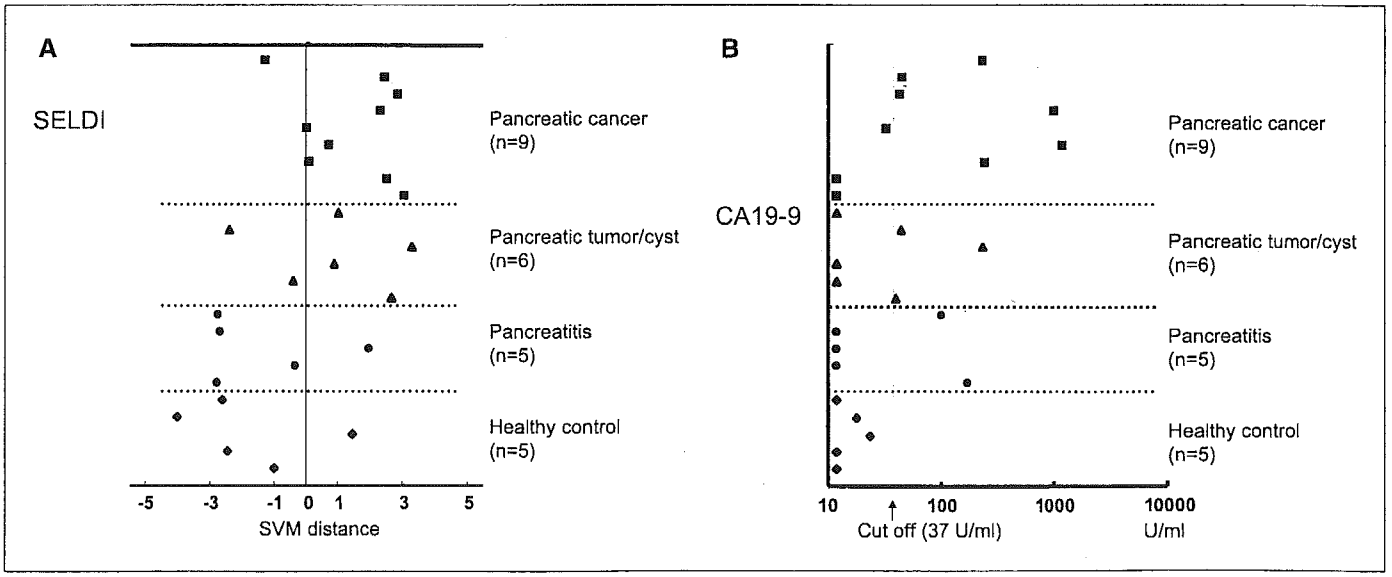

Figure 6. Confirmation in a second cohort treated at a different institution. *A*, calculated SVM distances of nine pancreatic cancer patients, six individuals with pancreatic tumors and/or cysts, five chronic pancreatitis patients, and five healthy controls seen at TMUH. *B*, plasma CA19-9 levels in nine pancreatic cancer patients, six individuals with pancreatic tumors and/or cysts, five chronic pancreatitis patients, and five healthy controls seen at TMUH. The cutoff value was set at 37 units/mL.

1982 (30), no single tumor marker applicable to the clinical diagnosis of pancreatic cancer has been identified. The carcinogenesis of pancreatic cancer is probably mediated via a variety of molecular pathways (2, 31), and multimarker analysis of proteins with different specificities is a realistic alternative to a conventional single biomarker assay.

There are pros and cons to SELDI-MS with high-resolution instruments. Although the primary goal of our study was the development of a bioassay applicable to the detection of pancreatic cancer, attempts to purify proteins from these four low-intensity peaks without contamination by neighboring high-intensity peaks have not been successful to date. However, the high reproducibility of QqTOF-MS warrants direct clinical application of its measurements and does not necessitate the actual protein identification of these peaks. Zhang et al. (12) reported that a set of three peaks, at 3,272, 12,828, and 28,043 *m/z*, could be used to detect early-stage ovarian cancer. The 28,043 *m/z* peak was down-regulated in ovarian cancer patients and was found to be derived from apolipoprotein A1. The relatively abundant 28,080 *m/z* protein identified as one of the peaks down-regulated in pancreatic cancer patients in this study (Table 3; Fig. 3) may be related to apolipoprotein A1. The mass deviation of 0.3% seen in the low-resolution TOF-MS may represent a drift in this region as large as 84 *m/z* (28,080 × 0.003 = 84). At least four peaks were detected between 28,000 and 28,100 *m/z* using the high-resolution QqTOF-MS instrument (Fig. 3). These peaks merged and were detected as a single peak with the low-resolution instrument (data not shown). The intensities of the 8,766, 17,272, and 14,779 *m/z* peaks were one magnitude smaller than that of the 28,080 *m/z* peak (Table 3) and were apparently below the sensitivity of tandem MS. So-called top-down proteomics using Fourier transform (FT)-MS (32) may be necessary to identify the proteins indicated by the low-intensity peaks of our classifier. However, an interface to the SELDI arrays is currently not available for FT-MS.

No significant differences in the detection rates for our classifier were observed among different stages of pancreatic cancer (Table 4). Koomen et al. (33) did plasma protein profiling of pancreatic cancer patients using MALDI-MS and identified a set of eight peaks distinguishing pancreatic cancer patients from controls with a sensitivity of 88% and a specificity of 75%. Protein identification revealed these peaks to be derived mainly from host response proteins. Many low molecular weight proteins detected by SELDI-MS in serum or plasma samples have also been reported to be metabolic products, proteolytic fragments, or peptide hormones. These proteins may not always be attributable to direct secretion or production by cancer cells, instead being the results of host responses in the microenvironment of the tumor (7, 18, 34), such as stromal desmoplastic reactions, inflammation, and angiogenesis. Two of eight pancreatic cancer patients who were classified as having "cancer," but none of normal controls in the TMUH validation cohort, had diabetes (data not shown). This raises the possibility that diabetic conditions, which are often associated with pancreatic cancer patients, also may influence the classifier.

All the pancreatic cancers were detected by complementary use of CA19-9 and/or the SELDI classifier (Table 5). CA19-9 is a tumor marker widely used for the evaluation of therapeutic effects and the detection of pancreatic cancer recurrence but is not considered to be applicable to mass screening (35–38). Ten percent to 15% of humans do not secrete CA19-9 because of their genetic Lewis antigen status (39). The CA19-9 level is often within reference range when pancreatic cancer is still at an early stage and is often elevated in benign biliary and pancreatic diseases. When the cutoff value for CA19-9 was set at 37 units/mL, which is widely used for clinical purposes, the false-positive rate of the combined CA19-9 and SELDI strategy reached 15.4% (Table 5). To increase diagnostic accuracy, the CA19-9 cutoff value may need to be adjusted and the selection of SELDI peaks may need to be further refined.

Early detection seems to be essential for improving the outcomes of pancreatic cancer patients. The SELDI classifier identified in this study has high potential for detecting pancreatic cancers (Tables 4 and 5), but one of the five pancreatitis patients in the TMUH validation cohort was classified into the pancreatic cancer category (Fig. 6). This pancreatitis patient may have a premalignant or preclinical condition and is currently being followed. Alternatively, because inflammatory conditions were not used in training, it is also possible that the classifier may not be entirely specific for the cancer phenotype. Machine learning was done with the training cohort, in which there were no cases with benign pancreatic diseases, because the discovery of biomarkers useful for pancreatic cancer screening in a large population made up mostly of healthy individuals was a primary goal of this study. The final diagnosis of pancreatic cancer is not made solely based on plasma protein profiling. CT, MRI, PET, ultrasound, and endoscopic and/or surgical approaches are employed as well. To evaluate the clinical significance of the biomarkers identified in this study and to refine the selection of biomarkers using a large number of subjects, including patients with pancreatic cancer and other pancreatic diseases, we need to undertake a prospective multi-institutional study.

Acknowledgments

Received 5/27/2005; revised 8/5/2005; accepted 9/9/2005.

Grant support: "Third Term Comprehensive Control Research for Cancer" from the Ministry of Health, Labor and Welfare; "Program for Promotion of Fundamental Studies in Health Sciences" of the National Institute of Biomedical Innovation of Japan; and Foundation for the Promotion of Cancer Research resident fellowship to Y. Hayashida (patent pending in Japan, no. 2005-070512).

The costs of publication of this article were defrayed in part by the payment of page charges. This article must therefore be hereby marked *advertisement* in accordance with 18 U.S.C. Section 1734 solely to indicate this fact.

We thank Drs. T. Kakizoe, N. Moriyama, and T. Yoshida (National Cancer Center) for helpful discussions and encouragement, Y. Ishiyama for her secretarial assistance, and Dr. K. Aoshima, H. Kuwabara, T. Isobe, and H. Matsuzuki (Mitsui Knowledge Industry) for the statistical analyses.

References

1. Yamamoto M, Ohashi O, Saitoh Y. Japan Pancreatic Cancer Registry: current status. Pancreas 1998;16:238–42.
2. Lowenfels AB, Maisonneuve P. Epidemiology and prevention of pancreatic cancer. Jpn J Clin Oncol 2004;34:238–44.
3. Landis SH, Murray T, Bolden S, Wingo PA. Cancer statistics, 1999. CA Cancer J Clin 1999;49:8–31.
4. Shimamura T, Sakamoto M, Ino Y, et al. Dysadherin overexpression in pancreatic ductal adenocarcinoma reflects tumor aggressiveness: relationship to e-cadherin expression. J Clin Oncol 2003;21:659–67.
5. Berrington de Gonzalez A, Darby S. Risk of cancer from diagnostic X-rays: estimates for the UK and 14 other countries. Lancet 2004;363:345–51.
6. Anderson NL, Anderson NG. The human plasma proteome: history, character, and diagnostic prospects. Mol Cell Proteomics 2002;1:845–67.
7. Issaq HJ, Veenstra TD, Conrads TP, Felschow D. The SELDI-TOF MS approach to proteomics: protein

profiling and biomarker identification. Biochem Biophys Res Commun 2002;292:587–92.
8. Chapman K. The ProteinChip Biomarker System from Ciphergen Biosystems: a novel proteomics platform for rapid biomarker discovery and validation. Biochem Soc Trans 2002;30:82–7.
9. von Eggeling F, Junker K, Fiedle W, et al. Mass spectrometry meets chip technology: a new proteomic tool in cancer research? Electrophoresis 2001;22:2898–902.
10. Petricoin EF, Ardekani AM, Hitt BA, et al. Use of proteomic patterns in serum to identify ovarian cancer. Lancet 2002;359:572–7.
11. Adam BL, Qu Y, Davis JW, et al. Serum protein fingerprinting coupled with a pattern-matching algorithm distinguishes prostate cancer from benign prostate hyperplasia and healthy men. Cancer Res 2002;62:3609–14.
12. Zhang Z, Bast RC, Jr., Yu Y, et al. Three biomarkers identified from serum proteomic analysis for the detection of early stage ovarian cancer. Cancer Res 2004;64:5882–90.
13. Banez LL, Prasanna P, Sun L, et al. Diagnostic potential of serum proteomic patterns in prostate cancer. J Urol 2003;170:442–6.
14. Baggerly KA, Morris JS, Coombes KR. Reproducibility of SELDI-TOF protein patterns in serum: comparing datasets from different experiments. Bioinformatics 2004;20:777–85.
15. Coombes KR, Morris JS, Hu J, Edmonson SR, Baggerly KA. Serum proteomics profiling-a young technology begins to mature. Nat Biotechnol 2005;23:291–2.
16. Ransohoff DF. Lessons from controversy: ovarian cancer screening and serum proteomics. J Natl Cancer Inst 2005;97:315–9.
17. Conrads TP, Fusaro VA, Ross S, et al. High-resolution serum proteomic features for ovarian cancer detection. Endocr Relat Cancer 2004;11:163–78.
18. Petricoin EF, Liotta LA. SELDI-TOF-based serum proteomic pattern diagnostics for early detection of cancer. Curr Opin Biotechnol 2004;15:24–30.
19. Koopmann J, Zhang Z, White N, et al. Serum diagnosis of pancreatic adenocarcinoma using surface-enhanced laser desorption and ionization mass spectrometry. Clin Cancer Res 2004;10:860–8.
20. Japanese Pancreas Society. General rule for the study of pancreatic cancer. Tokyo: Kanehara Shuppan; 2002.
21. Hara T, Honda K, Ono M, Naito K, Hirohashi S, Yamada T. Identification of two serum biomarkers of renal cell carcinoma by surface-enhanced laser desorption/ionization mass spectrometry. J Urol 2005;174:1213–7.
22. Hayashida Y, Honda K, Osaka Y, et al. Possible prediction of chemoradiosensitivity of esophageal cancer by serum protein profiling. Clin Cancer Res. In press.
23. Metz CE. Basic principles of ROC analysis. Semin Nucl Med 1978;8:283–98.
24. Byvatov E, Schneider G. Support vector machine applications in bioinformatics. Appl Bioinformatics 2003;2:67–77.
25. Kadota K, Nishimura S, Bono H, et al. Detection of genes with tissue-specific expression patterns using Akaike's information criterion procedure. Physiol Genomics 2003;12:251–9.
26. Tolson J, Bogumil R, Brunst E, et al. Serum protein profiling by SELDI mass spectrometry: detection of multiple variants of serum amyloid α in renal cancer patients. Lab Invest 2004;84:845–56.
27. Howard BA, Wang MZ, Campa MJ, Corro C, Fitzgerald MC, Patz EF, Jr. Identification and validation of a potential lung cancer serum biomarker detected by matrix-assisted laser desorption/ionization-time of flight spectra analysis. Proteomics 2003;3:1720–4.
28. Weinstein PS, Skinner M, Sipe JD, Lokich JJ, Zamcheck N, Cohen AS. Acute-phase proteins or tumour markers: the role of SAA, SAP, CRP and CEA as indicators of metastasis in a broad spectrum of neoplastic diseases. Scand J Immunol 1984;19:193–8.
29. Khan N, Cromer CJ, Campa M, Patz EF, Jr. Clinical utility of serum amyloid A and macrophage migration inhibitory factor as serum biomarkers for the detection of nonsmall cell lung carcinoma. Cancer 2004;101:379–84.
30. Herlyn M, Sears HF, Steplewski Z, Koprowski H. Monoclonal antibody detection of a circulating tumor-associated antigen. I. Presence of antigen in sera of patients with colorectal, gastric, and pancreatic carcinoma. J Clin Immunol 1982;2:135–40.
31. Gansauge S, Gansauge F, Beger HG. Molecular oncology in pancreatic cancer. J Mol Med 1996;74:313–20.
32. Gershon D. Proteomics technologies: probing the proteome. Nature 2003;424:581–7.
33. Koomen JM, Shih LN, Coombes KR, et al. Plasma protein profiling for diagnosis of pancreatic cancer reveals the presence of host response proteins. Clin Cancer Res 2005;11:1110–8.
34. Liotta LA, Ferrari M, Petricoin E. Clinical proteomics: written in blood. Nature 2003;425:905.
35. Goggins M, Canto M, Hruban R. Can we screen high-risk individuals to detect early pancreatic carcinoma? J Surg Oncol 2000;74:243–8.
36. Abrams RA, Grochow LB, Chakravarthy A, et al. Intensified adjuvant therapy for pancreatic and periampullary adenocarcinoma: survival results and observations regarding patterns of failure, radiotherapy dose and CA19-9 levels. Int J Radiat Oncol Biol Phys 1999;44:1039–46.
37. Ritts RE, Pitt HA. CA 19-9 in pancreatic cancer. Surg Oncol Clin N Am 1998;7:93–101.
38. Safi F, Schlosser W, Kolb G, Beger HG. Diagnostic value of CA 19-9 in patients with pancreatic cancer and nonspecific gastrointestinal symptoms. J Gastrointest Surg 1997;1:106–12.
39. Narimatsu H, Iwasaki H, Nakayama F, et al. Lewis and secretor gene dosages affect CA19-9 and DU-PAN-2 serum levels in normal individuals and colorectal cancer patients. Cancer Res 1998;58:512–8.

膵癌に対する治療方針と治療法の選択について：内科的立場から

奥坂　拓志
国立がんセンター中央病院肝胆膵内科

はじめに

わが国の膵癌による死亡数は、年間2万人を超えており、癌死亡者数の第5位を占めている[1]。膵癌は、最も難治性の癌の1つであり、画像診断が発達した現在でも、多くの例が進行癌の状態で診断され、また切除例においても術後早期に再発することが少なくない。

このような膵癌の予後を改善させるためには、確実な早期診断法の確立や、有効な非手術療法の開発などが重要である。本稿では、膵癌の大部分を占める浸潤性膵管癌(以後、膵癌とする)に対する非手術療法について、科学的根拠に基づいてその選択法や治療法をまとめた。

治療法とその選択

膵癌に対する非手術療法としては、放射線療法(体外照射、術中照射など)、化学療法(全身性投与、局所投与)、内分泌療法、免疫療法、温熱療法などや放射線化学療法などの併用療法が挙げられるが、遠隔転移の明らかでない切除不能局所進行例に対しては、後述する無作為化比較試験の成績から放射線化学療法が標準的治療法と位置付けられている。また、遠隔転移を有する症例に対しては主としてgemcitabineによる全身性化学療法が行われている(図)。

進行膵癌に対する化学療法

疼痛や全身状態の悪化などの症状が高率にみられる膵癌では、化学療法によってそれらの症状が改善することは重要であり、症状緩和効果を主要評価項目として、gemcitabineと5-FUの無作為化比較試験が行われた[2]。gemcitabine群では、症状緩和効果が24%(15/63例)にみられ、5-FU群の5%(3/63例)に比べ有意に高率であった。さらに、50%生存期間もgemcitabine群では5.7カ月、5-FU群では4.4カ月とgemcitabine群で有意に良好であった。わが国でもgemcitabineを用いた臨床試験が実施され、膵癌に対する保険適用が承認された[3]。この結果、わが国においてもgemcitabineは進行膵癌に対する第一選択の薬剤として位置付けられ、現在臨床の現場においても広く用いられている。

また、gemcitabineの開発後、marimastatやBAY12-9566(いずれもmatrix metalloproteinase inhibitor)、exatecan(topoisomerase I inhibitor)といった新しい抗癌剤とgemcitabineとの無作為化比較試験がそれぞれ実施されているが、いずれの生存期間もgemcitabine群が有意に良好、あるいは、良好な傾向を示し、現在までのところgemcitabineを凌駕する薬剤は登場していない(表1)。

単剤で優れた治療成績を示したgemcitabineは、5-FU、cisplatin、irinotecan(CPT-11)、marimastat、tipifarnib(R115777、farnesyl transferase inhibitor)、oxaliplatin、pemetrexed、exate-

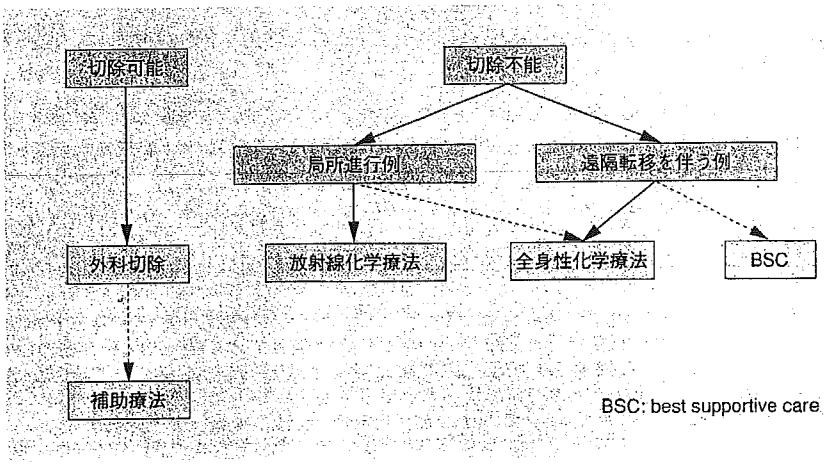

図　膵癌の主な治療法のアルゴリズム

表1　Gemcitabineと他の薬剤(単剤)との無作為化比較試験

報告者 報告年	治療法	症例数	生存期間中央値 (月)	P
Burris 1997	Gem 5-FU	63 63	5.7 4.4	0.0025
Moore 2000	Gem BAY12-9566	両群で 277	6.4 3.2	0.0001
Bramhall 2001	Gem Marimastat 5mg Marimastat 10mg Marimastat 25mg	103 104 105 102	5.6 3.7 3.5 4.2	0.163 0.045 0.78
Cheverton 2004	Gem Exatecan	170 169	6.6 5	0.09

5-FU: fluorouracil
Gem: gemcitabine

canなどの薬剤とそれぞれ併用され、gemcitabine単独との無作為化比較試験が実施されている。いずれの試験においても両群の生存期間には有意な差を認めていない。

最近、gemcitabineとerlotinib併用療法の生存期間がgemcitabineを有意に凌駕したと報告されたが、その生存期間中央値の差は2週間であり、本併用療法を標準的治療法と位置付けるかに関しては十分なコンセンサスは得られていない(表2)。

以上のように、現在までのところ、gemcitabine単独療法を明らかに上回る治療法は確立しておらず、gemcitabine単独療法は、多くの施設で第一選択療法として広く用いられている。しかし、gemcitabineの登場以来、膵癌化学療法に対する関心が急速に高まっており、国内外で多くの臨床試験が進行している。海外では、bevacizumabやcetuximabなどの分子標的治療薬を用いた大規模比較試験が進められている。わが国では、CPT-11やS-1の臨床試験が実施され、比較的高い奏効率が報告されている。近い将来において、gemcitabine単独療法を凌駕する、より有効な治療法が確立するものと期待されている。

切除不能局所進行例に対する治療法の選択

明らかな遠隔転移を認めない局所進行膵癌例に対しては、これまでに欧米において放射線化学療法と、放射線療法単独あるいは化学療法単独とを比較する4つの無作為化比較試験が行われている[4-7]。そのうちの3つの試験において、放射線化学療法は単独療法に比べ有意に良好な遠隔成績を示しており、局所進行膵癌に対しては放射線化学療法が標準的治療法と位置付けられている。

これらの比較試験で用いられた放射線化学療法は、5-FUが主に放射線増感剤としてbolusで投与され、放射線は40～60Gyの体外照射が用いられている。最近では、化学療法剤としての効果の増強と副作用の軽減を期待して5-FUは持続投与で用いられる傾向にある。

近年、海外で実施される化学療法の臨床試験には、遠隔転移例のほかに局所進行例も対象として含めることがある。これらの試験のサブセット解析において、gemcitabine治療を受けた局所進行例の比較的良好な遠隔成績が報告されており、実地臨床においても局所進行例にもgemcitabineによる化学療法を実施する場合がある[8]。しかし、局所進行例において、放射線化学療法とgemcitabineとを比較する無作為化比較試験の報告はなく、gemcitabineによる化学療法を局所進行例に対する標準的治療法とするには、さらなるエビデンスの積み重ねが必要と考えられる。

切除例に対する術後補助療法

術後補助療法に関する無作為化比較試験もこれまでに数本行われている。米国のGastrointestinal Tumor Study Group (GITSG)は、放射線化学療法と無治療とを比較し、術後補助放射線化学療法群の生存期間が有意に良好であることを報告した。しかし、European Organisation

表2　Gemcitabineを中心とした多剤併用療法に関する主な無作為化比較試験

報告者 報告年	治療法	症例数	生存期間中央値 (月)	P
Berlin 2002	Gem Gem、5-FU	162 160	5.4 6.7	0.09
Richards 2004	Gem Gem、Pemetrexed	282 283	6.3 6.2	0.72
Colucci 2002	Gem Gem、CDDP	54 53	5.0 7.5	0.43
Heinemann 2003	Gem Gem、CDDP	100 98	6.0 7.6	0.12
Louvet 2004	Gem Gem、Oxaliplatin	156 157	7.1 9.0	0.13
Lima 2003	Gem Gem、CPT-11	180 180	6.6 6.3	0.789
O'Reilly 2004	Gem Gem、Exatecan	174 175	6.2 6.7	0.52
Bramhall 2002	Gem Gem、Marimastat	119 120	5.5 5.5	0.99
Van Cutsem 2002	Gem Gem、R115777	347 341	6.1 6.4	0.75
Moore 2003	Gem Gem、Erlotinib	284 285	5.9 6.4	0.03

5-FU: fluorouracil
CDDP: cisplatin
CPT-11: irinotecan
Gem: gemcitabine

for Research and Treatment of Cancer (EORTC) による無作為化比較試験では、放射線化学療法群と無治療群との間には有意差を認めていない。

補助化学療法については、AMF療法(doxorubicin、mitomycin C、5-FU)群が無治療群に比べ有意に良好な生存期間を示している。European Study Group for Pancreatic Cancer(ESPAC)により実施された比較試験では、化学療法(5-FU、leucovorin)では有意な延命効果を認めたが、放射線化学療法では延命効果がみられなかった。

わが国においても5-FU＋mitomicin C併用療法、あるいは5-FU＋cisplatin併用療法をそれぞれ無治療と比較した無作為化比較試験が実施されたが、有意な差は認めていない。最近、5-FUをベースとする術後補助化学療法の有用性を示すメタアナリシスが英国より報告された[9]が、わが国においてはこれを支持する高いエビデンスの報告が乏しく、現時点では十分なコンセンサスが得られていない。現在、gemcitabineによる術後補助化学療法について比較試験が行われており、その成果が待たれている。

おわりに

症状緩和効果、延命効果を有し、毒性の比較的軽微なgemcitabineの登場は、膵癌化学療法に大きな変化をもたらした。しかし、膵癌患者の予後はいまだ不良であり、その克服に向けて分子標的治療薬などの新たな抗癌剤の開発が進められている。今後、これらの臨床試験を効率的に進めることによって、より有効な治療法が確立するものと期待されている。

文　献

1) 厚生労働省大臣官房統計情報部: 平成14年人口動態統計, 東京 : 284-285, 2004.
2) Burris HA 3rd, Moore MJ, Andersen J, et al: Improvements in survival and clinical benefit with gemcitabine as first-line therapy for patients with advanced pancreas cancer: a randomized trial. J Clin Oncol 15: 2403-2413, 1997.
3) Okada S, Ueno H, Okusaka T, et al: Phase I trial of gemcitabine in patients with advanced pancreatic cancer. Jap J Clin Oncol 31: 7-12, 2001.
4) Moertel CG, Childs DS, Reitemeier RJ, et al: Combined 5-fluorouracil and supervoltage radiation therapy of locally unresectable gastrointestinal cancer. Lancet 2: 865-867, 1969.
5) Moertel CG, Frytak S, Hahn RG, et al: Therapy of locally unresectable pancreatic carcinoma. A randomized comparison of high dose (6000 Rads) radiation alone, moderate dose radiation (4000 Rads +5-fluorouracil), and high dose radiation +5-fluorouracil.The Gastrointestinal Tumor Study Group. Cancer 48: 1705-1710, 1981.
6) Klaassen DJ, MacIntyre JM, Catton GE, et al: Treatment of locally unresectable cancer of the stomach and pancreas: A randomized comparison of 5-fluorouracil alone with radiation plus concurrent and maintenance 5-fluorouracil.An Eastern Cooperative Oncology Group Study. J Clin Oncol 3: 373-378, 1985.
7) Gastrointestinal Tumor Study Group: Treatment of locally unresectable carcinoma of the pancreas: Comparison of combined-modality therapy (chemotherapy plus radiotherapy) to chemotherapy alone. J Natl Cancer Inst 80: 751-755, 1988.
8) Rocha Lima CM, Green MR, Rotche R, et al: Irinotecan plus gemcitabine results in no survival advantage compared with gemcitabine monotherapy in patients with locally advanced or metastatic pancreatic cancer despite increased tumor response rate. J Clin Oncol 22:3776-3783, 2004.
9) Stocken DD, Buchler MW, Dervenis C, Bassi C, Jeekel H, Klinkenbijl JH, Bakkevold KE, Takada T, Amano H, Neoptolemos JP: Meta-analysis of randomised adjuvant therapy trials for pancreatic cancer. Br J Cancer 92:1372-81, 2005.

切除不能膵癌に対する化学療法，放射線療法

上野秀樹・奥坂拓志
国立がんセンター中央病院肝胆膵内科／うえの・ひでき　おくさか・たくじ

はじめに

わが国では年間約2万人が膵癌のために死亡しており，これは癌による死因の第5位を占めている．膵癌を根治する治療は切除術しかないが，診断技術が進歩した現在でも8割以上の患者は切除不能な進行癌の状態で発見されており，その予後はきわめて不良である．膵癌患者の予後改善のためには，早期診断技術の向上とともに非切除療法の進歩が必要である．

切除不能膵癌は治療戦略上，明らかな遠隔転移を認めないが周囲への浸潤のために切除できない局所進行膵癌と，遠隔転移を有する膵癌に分けられ，局所進行膵癌に対しては放射線化学療法または化学療法が，遠隔転移を有する膵癌に対しては化学療法が，延命や症状緩和効果を目的として行われている．本稿では，進行膵癌に対するこれらの非切除療法の現状と展望について解説する．

化学療法

1. 化学療法の対象

局所進行膵癌に関しては過去の比較試験の結果，放射線化学療法が標準治療として認識されており(放射線療法の項参照)，遠隔転移を伴った膵癌が化学療法の良い対象である．しかし遠隔転移を有する患者は全身状態が悪いことが多く，そのような例は一般に治療抵抗性で予後不良であることから化学療法の適応は慎重に行う．当院では，日常の大半を臥床して過ごす例(performance status 3以上)，経口摂取が不良な例，減黄不能な黄疸や多量の腹水を有する例，などに対しては緩和ケアを勧めている．実際に化学療法を行う際は，治療内容や副作用について十分に説明し，患者本人の同意を得ることが大切である．また，治療前に組織学的診断がなされていることが望ましい．

2. 化学療法の実際

膵癌に対しては従来5-fluorouracil(5-FU)を中心とした化学療法が行われていたが，その治療成績は満足できるものではなかった．近年，海外で膵癌の初回化学療法例を対象にgemcitabine(ジェムザール®)と5-FUの無作為化比較試験が行われ，gemcitabine群の方が，症状緩和効果および生存期間に関して有意に優れていたことが報告された[1]．その後の臨床試験でも膵癌に対するgemcitabineの効果が報告されており，gemcitabineは現在，進行膵癌に対する第一選択の抗癌剤と考えられている．週1回，1,000 mg/m^{2}のgemcitabineを30分かけて点滴静注し，3週間投与したら1週間休薬するパターンを1コースとして，病態が増悪しない限り継続する方法が一般的である．gemcitabineの主な副作用は，骨髄抑制，悪心・嘔吐，食欲低下，倦怠感，皮疹，肝機能障害などであるが，軽度なことが多く，通常は外来での治療が可能である．間質性肺炎はまれな副作用であるが，投与中に咳や息切れなどが出現した場合はX線などで胸部を確認する．gemcitabine投与日に診察と血液生化学的検査を行い，異常の程度によっては，減量や休薬を考慮する．投与当日の好中球数が1,000/mm^{3}未満または血小板数が70,000/mm^{3}未満であれば，骨髄機能が回復するまで投与を延期する．前投薬は必要ないことが多いが，悪心や皮疹を認める場合はセロトニン受容体拮抗剤(カイトリル®)やステロイドを併用する．進行膵癌に対するgemcitabine単剤の奏効率は5～15%程度であり，5～6ヵ月前後の生存期間中央値(MST)が報告されている．

3. 新しい化学療法

a. gemcitabine定速静注法

gemcitabineは代謝拮抗剤に分類される抗癌剤で，細胞内でdeoxycytidine kinaseによってリ